Electronic Supplementary Information

In situ transformations of Pd/NHC complexes with N-heterocyclic carbene ligands of different nature into colloidal Pd nanoparticles

Alexander Yu. Kostyukovich,[a] Andrey M. Tsedilin,[a] Ekaterina D. Sushchenko,[a] Dmitry B. Eremin,[a] Alexey S. Kashin,[a] Maxim A. Topchiy,[b,c] Andrey F. Asachenko,[b,c] Mikhail S. Nechaev[b,c] and Valentine P. Ananikov[a,b*]

[a] Zelinsky Institute of Organic Chemistry, Russian Academy of Sciences, Leninsky Pr. 47, Moscow 119991, Russia. E-mail: val@ioc.ac.ru

[b] M. V. Lomonosov Moscow State University, Leninskie Gory 1 (3), Moscow, 119991, Russia

[c] A. V. Topchiev Institute of Petrochemical Synthesis, Russian Academy of Sciences, Leninsky Prospect 29, Moscow, 119991, Russia

Content

***BIMe** complexes*

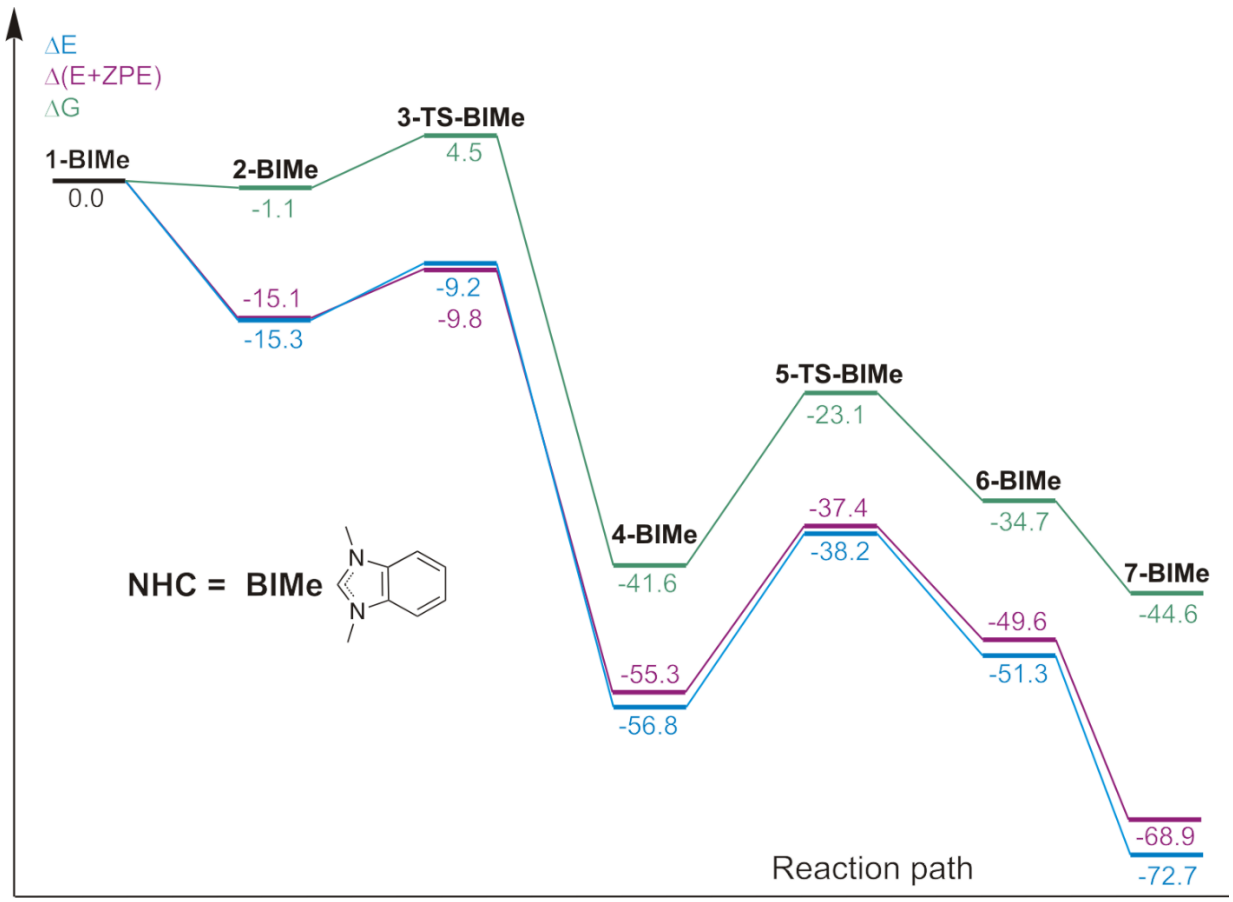

Figure S1. ΔE, Δ(E+ZPE) and ΔG potential energy surfaces for the PhI oxidative addition and subsequent Ph-NHC coupling for the **BIMe** complexes. PBE1PBE/6-311+G(d)&SDD level of theory.

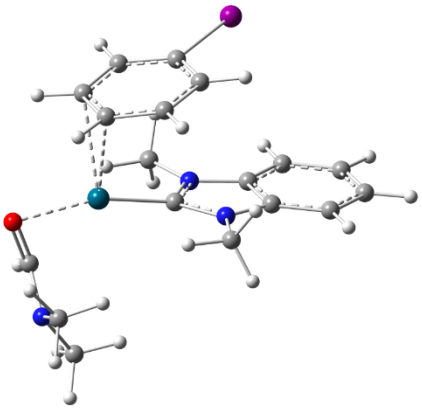

2a-BIMe

ΔE = 0; Δ(E+ZPE) = 0; ΔG = 0 kcal/mol

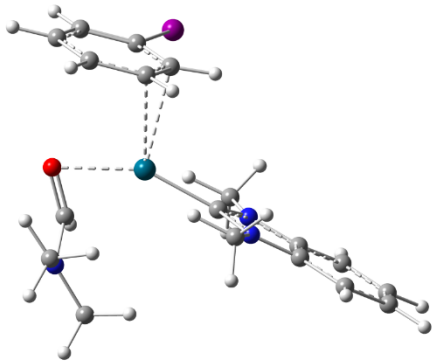

2b-BIMe

ΔE = 4.2; Δ(E+ZPE) = 3.9; ΔG = 2.7 kcal/mol

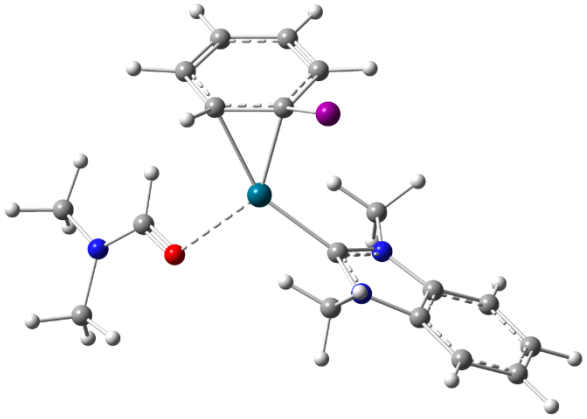

2c-BIMe

ΔE = 1.8; Δ(E+ZPE) = 1.4; ΔG = -0.7 kcal/mol

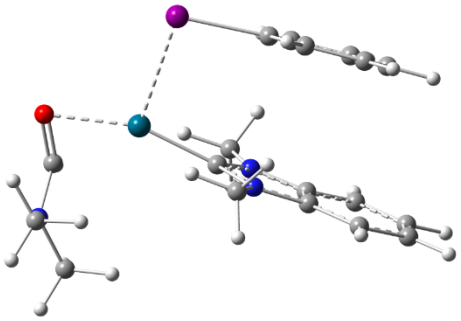

2d-BIMe

ΔE = 1.2; Δ(E+ZPE) = 1.3; ΔG = 0.7 kcal/mol

Figure S2. Energies and optimized structures of **2-BIMe** isomers.

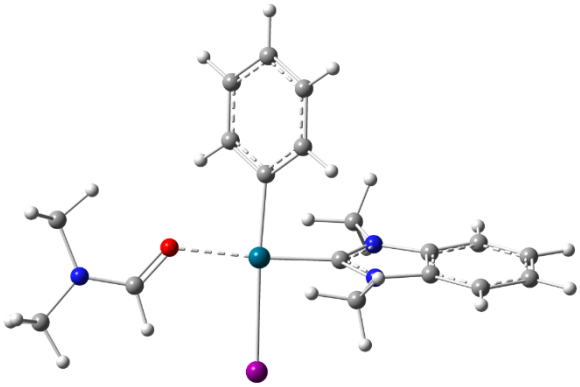

4a-BIMe

ΔE = 0; Δ(E+ZPE) = 0; ΔG = 0 kcal/mol

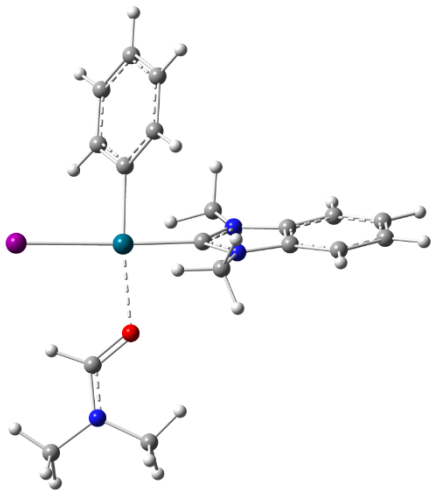

4b-BIMe

ΔE = 4.0; Δ(E+ZPE) = 4.0; ΔG = 4.2 kcal/mol

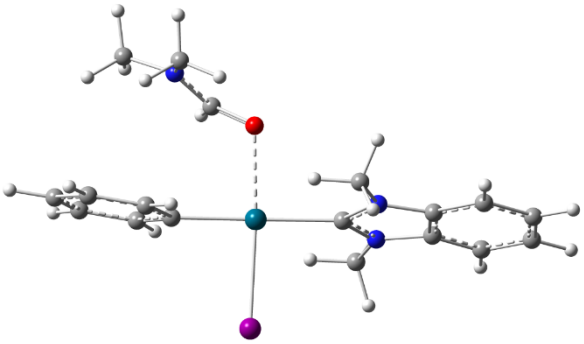

4c-BIMe

ΔE = 14.8; Δ(E+ZPE) = 14.5; ΔG = 14.8 kcal/mol

Figure S3. Energies and optimized structures of **4-BIMe** isomers.

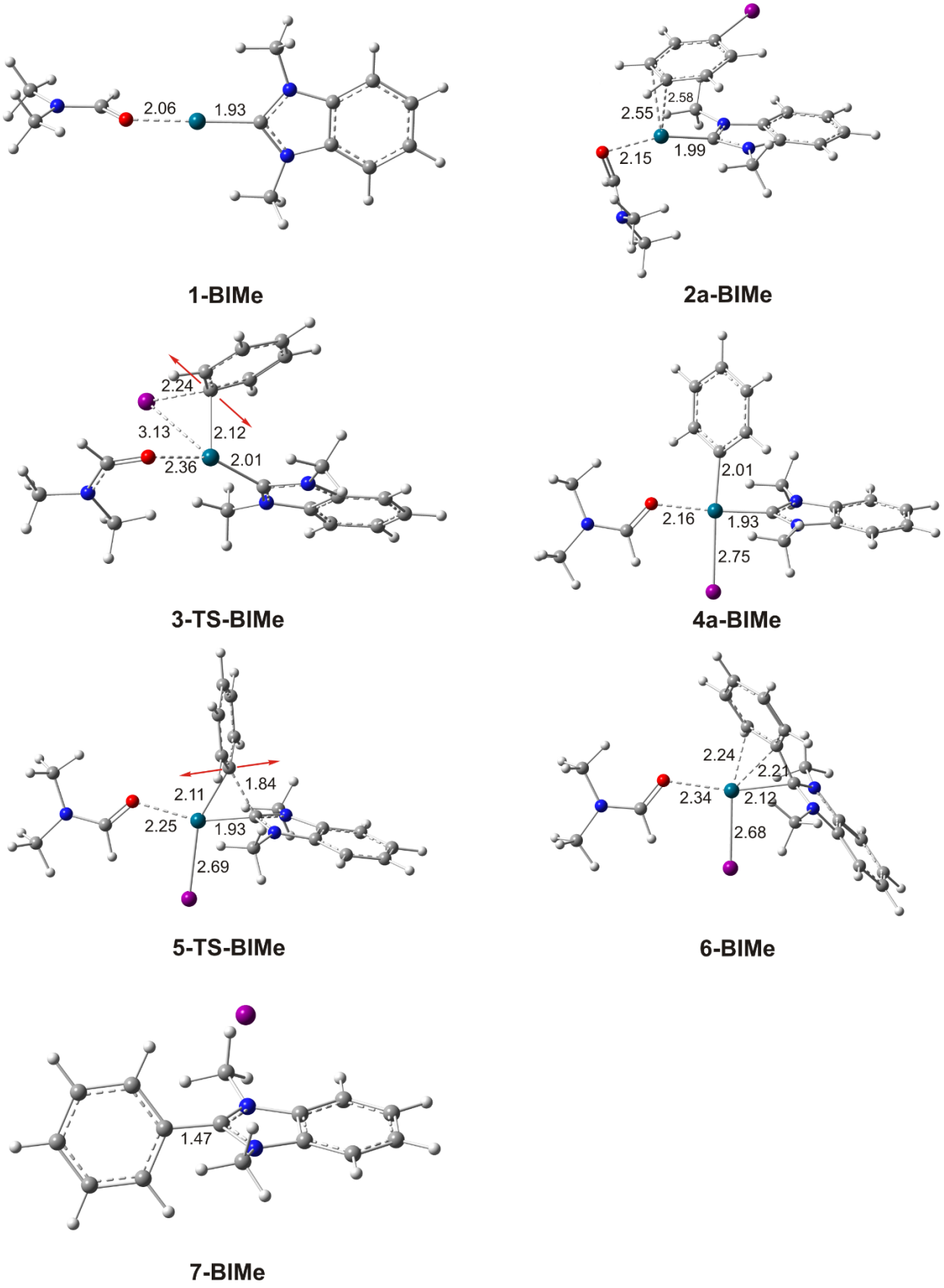

Figure S4. Optimized structures and selected bond distances (in angstroms) for **1-BIMe** – **7-BIMe** complexes. The atomic movements corresponding to the imaginary frequencies are depicted by red arrows.

***IMe** complexes*

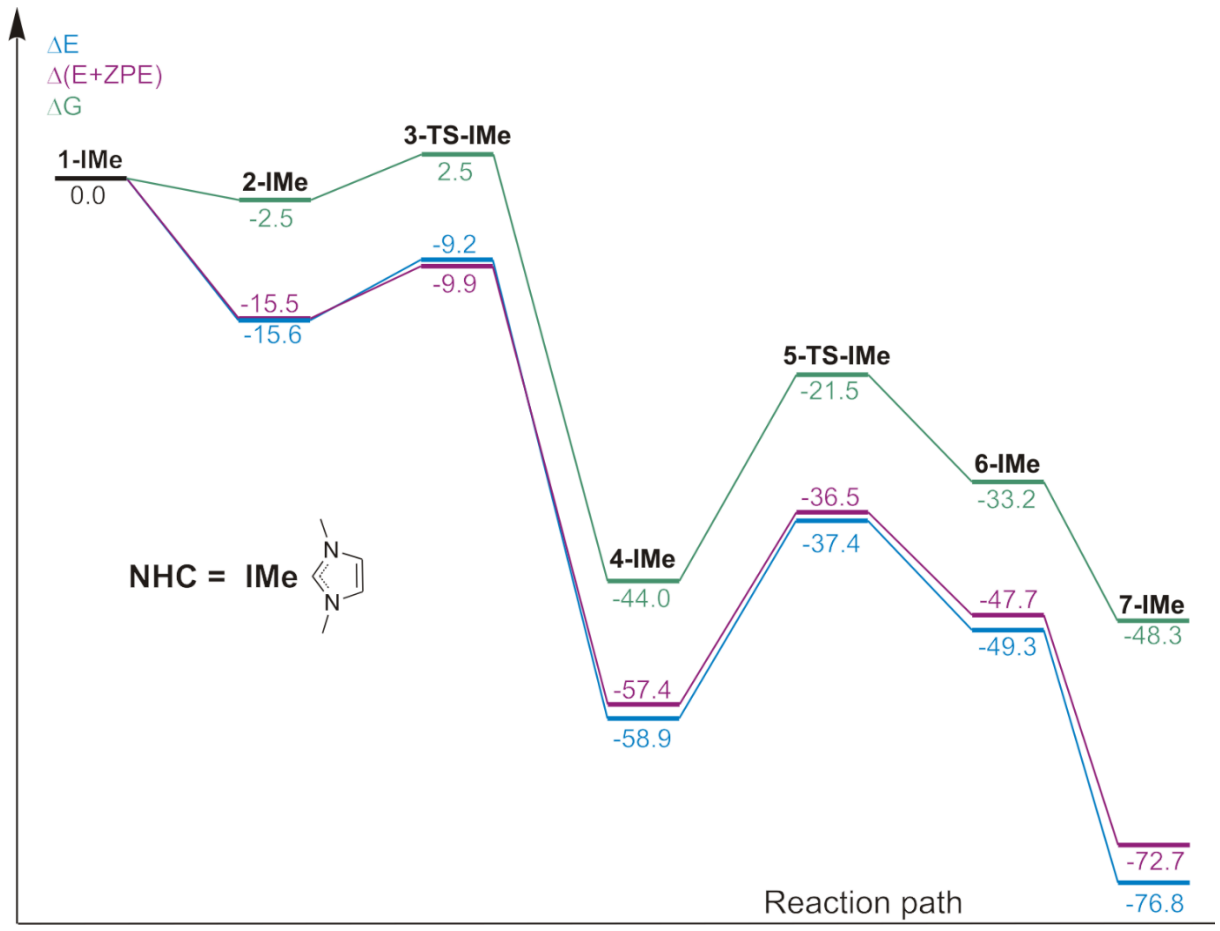

Figure S5. ΔE, Δ(E+ZPE) and ΔG potential energy surfaces for the PhI oxidative addition and subsequent Ph-NHC coupling for the **IMe** complexes. PBE1PBE/6-311+G(d)&SDD level of theory.

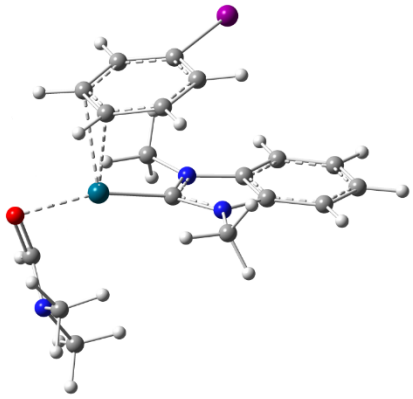

2a-IMe

ΔE = 0; Δ(E+ZPE) = 0; ΔG = 0 kcal/mol

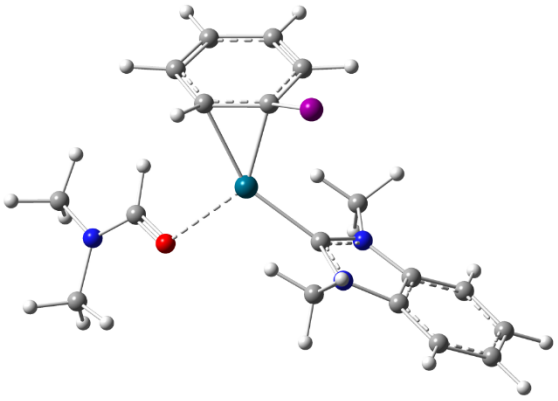

2c-IMe

ΔE = 0.9; Δ(E+ZPE) = 0.6; ΔG = -1.4 kcal/mol

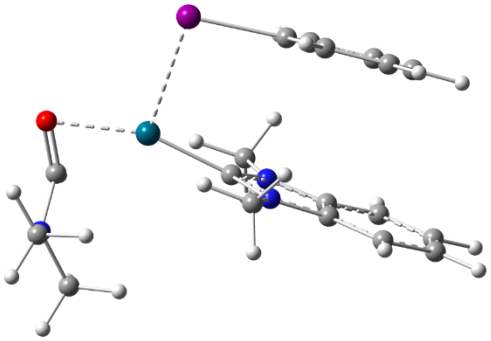

2d-IMe

ΔE = 1.8; Δ(E+ZPE) = 2.2; ΔG = -1.7 kcal/mol

Figure S6. Energies and optimized structures of **2-IMe** isomers.

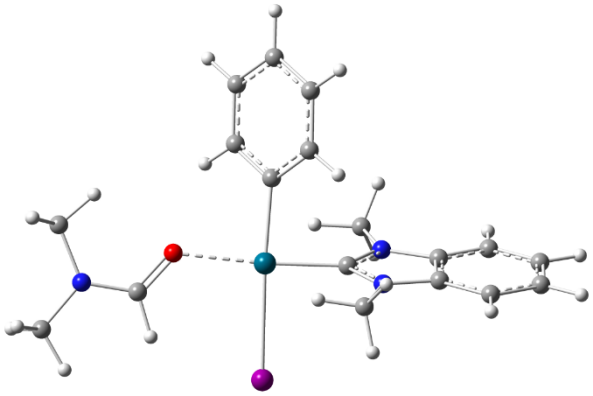

4a-IMe

ΔE = 0; Δ(E+ZPE) = 0; ΔG = 0 kcal/mol

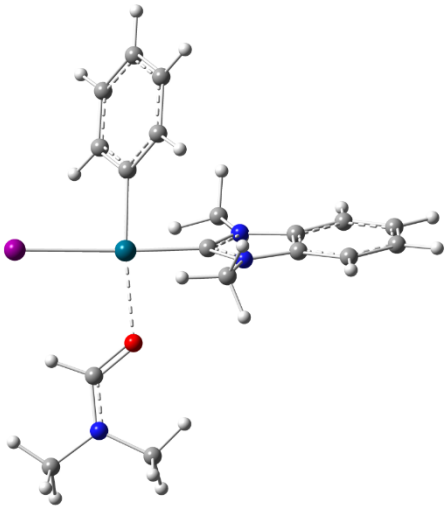

4b-IMe

ΔE = 4.0; Δ(E+ZPE) = 4.1; ΔG = 4.8 kcal/mol

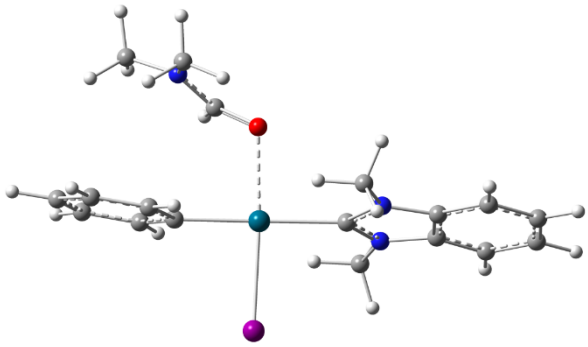

4c-IMe

ΔE = 14.3; Δ(E+ZPE) = 14.0; ΔG = 13.8 kcal/mol

Figure S7. Energies and optimized structures of **4-IMe** isomers.

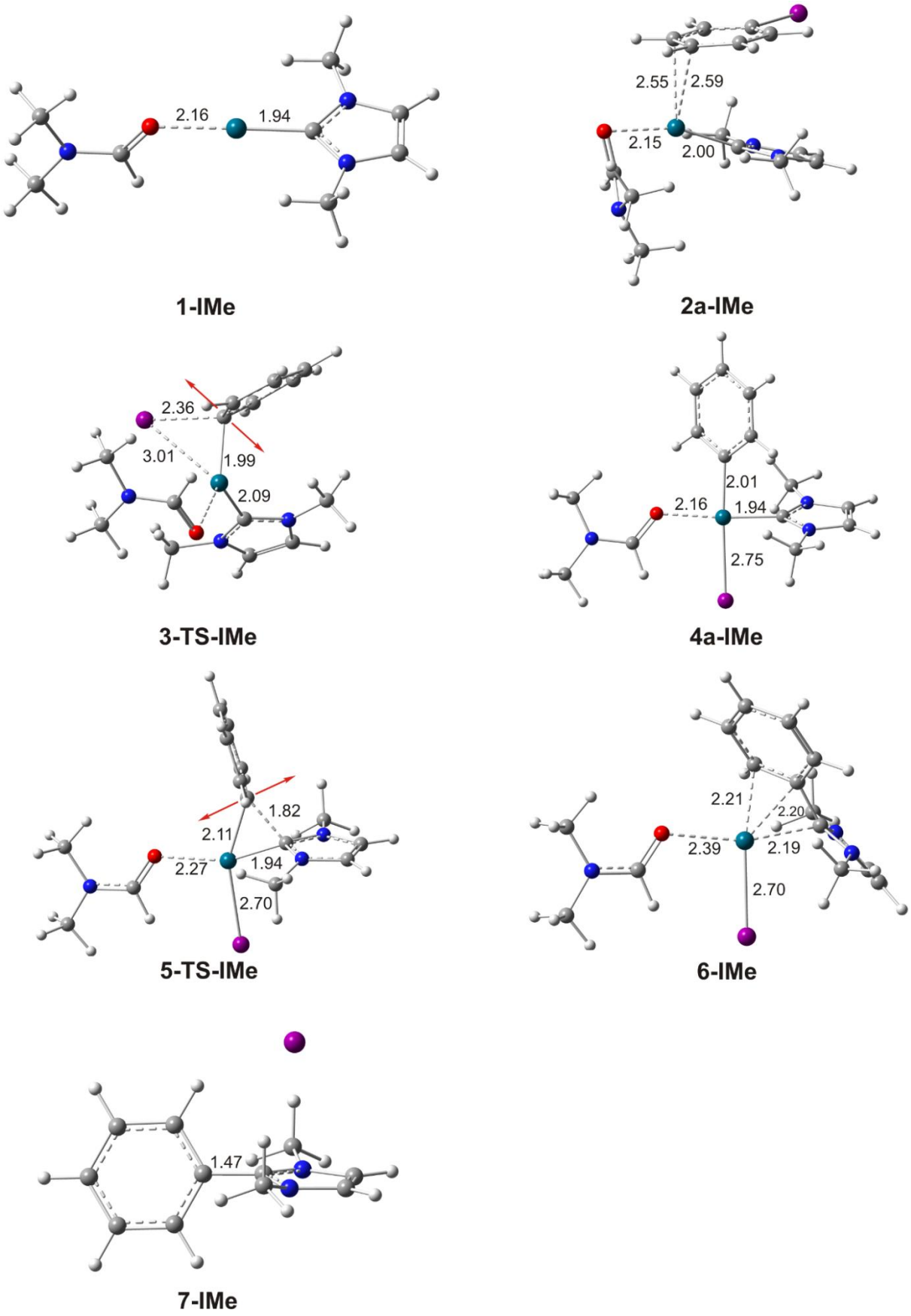

Figure S8. Optimized structures and selected bond distances (in angstroms) for **1-IMe** – **7-IMe** complexes. The atomic movements corresponding to the imaginary frequencies are depicted by red arrows.

***SIMe** complexes*

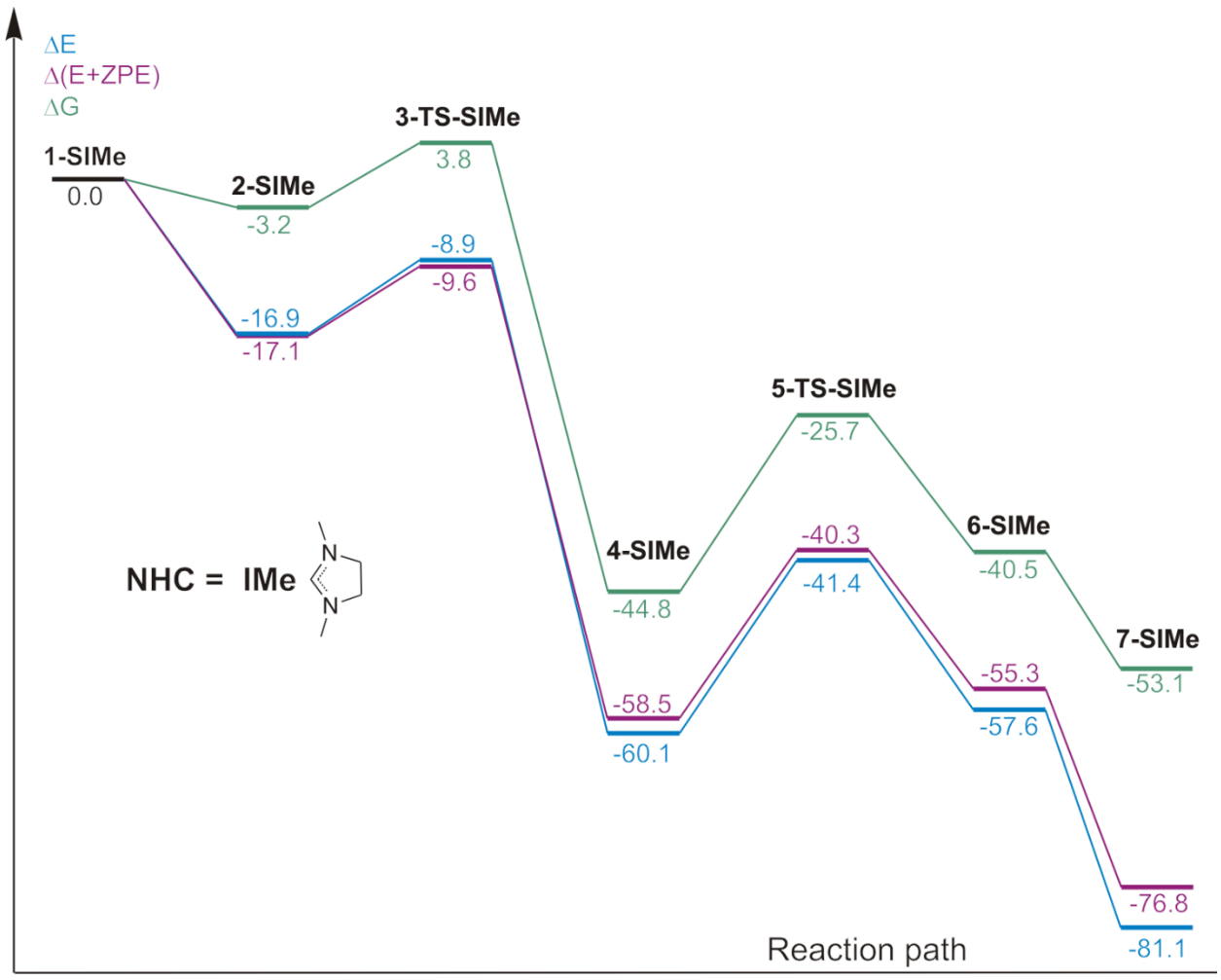

Figure S9. ΔE, Δ(E+ZPE) and ΔG potential energy surfaces for the PhI oxidative addition and subsequent Ph-NHC coupling for the **SIMe** complexes. PBE1PBE/6-311+G(d)&SDD level of theory.

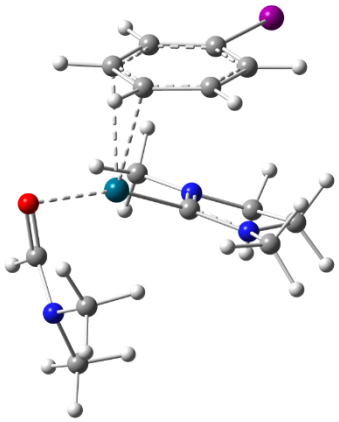

2a-SIMe

ΔE = 0; Δ(E+ZPE) = 0; ΔG = 0 kcal/mol

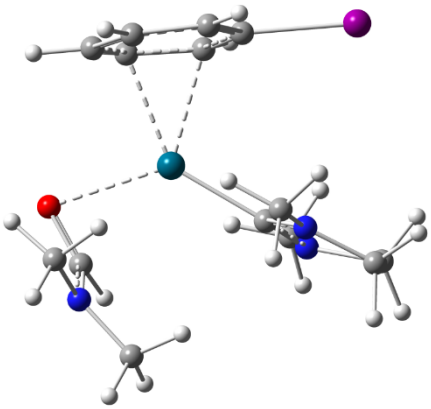

2b-SIMe

ΔE = -0.4; Δ(E+ZPE) = -0.7; ΔG = -1.0 kcal/mol

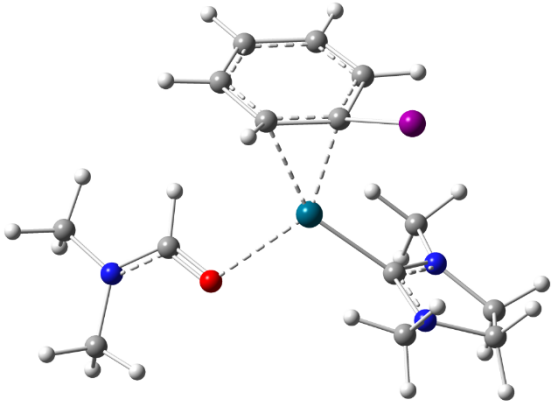

2c-SIMe

ΔE = 1.6; Δ(E+ZPE) = 1.4; ΔG = -0.2 kcal/mol

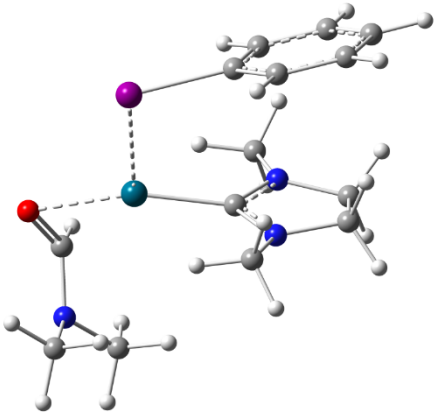

2d-SIMe

ΔE = 2.5; Δ(E+ZPE) = 2.7; ΔG = 2.5 kcal/mol

Figure S10. Energies and optimized structures of **2-SIMe** isomers.

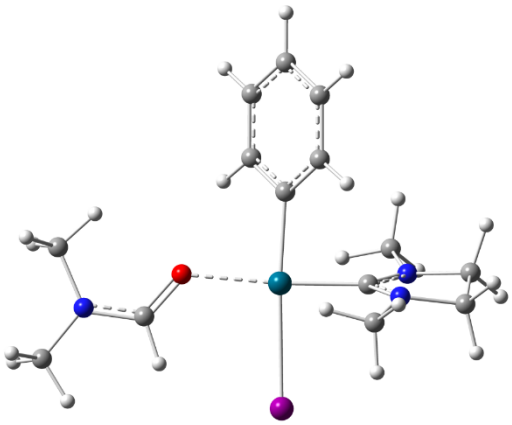

4a-SIMe

ΔE = 0; Δ(E+ZPE) = 0; ΔG = 0 kcal/mol

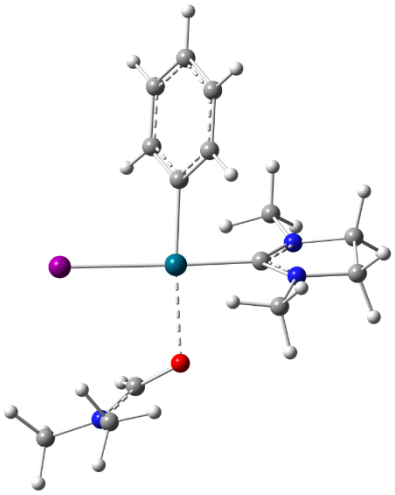

4b-SIMe

ΔE = 5.0; Δ(E+ZPE) = 4.9; ΔG = 5.4 kcal/mol

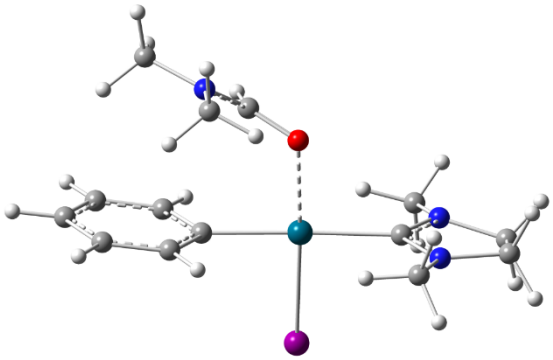

4c-SIMe

ΔE = 15.7; Δ(E+ZPE) = 15.2; ΔG = 14.7 kcal/mol

Figure S11. Energies and optimized structures of **4-SIMe** isomers.

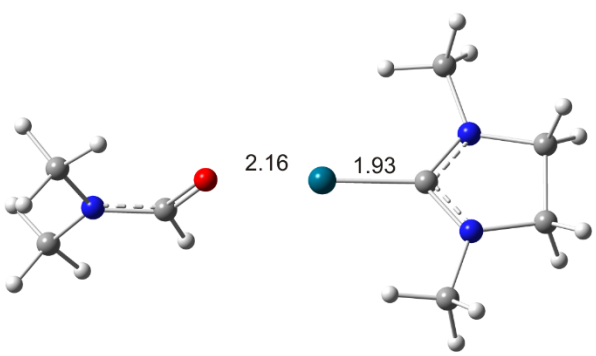

1-SIMe

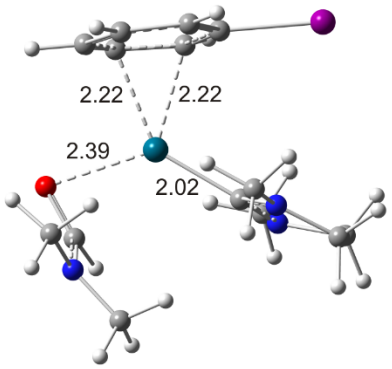

2b-SIMe

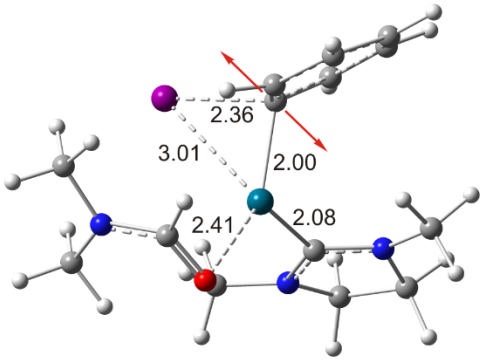

3-TS-SIMe

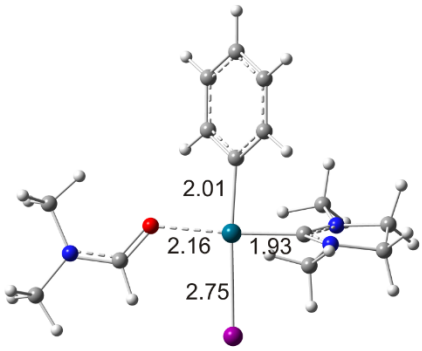

4a-SIMe

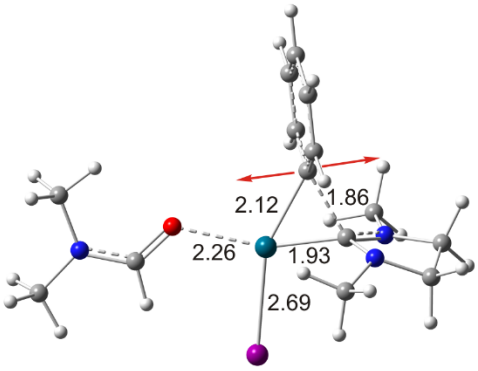

5-TS-SIMe

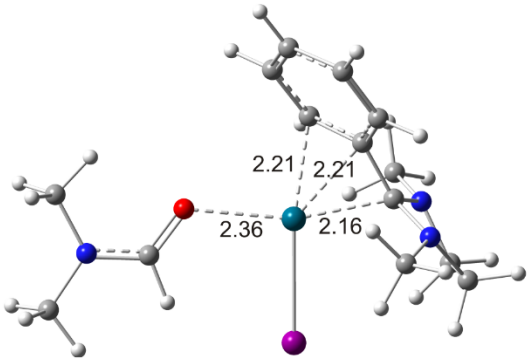

6-SIMe

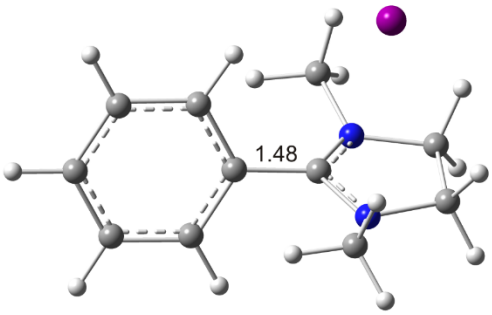

7-SIMe

Figure S12. Optimized structures and selected bond distances (in angstroms) for **1-SIMe** – **7-SIMe** complexes. The atomic movements corresponding to the imaginary frequencies are depicted by red arrows.

***PIMe** complexes*

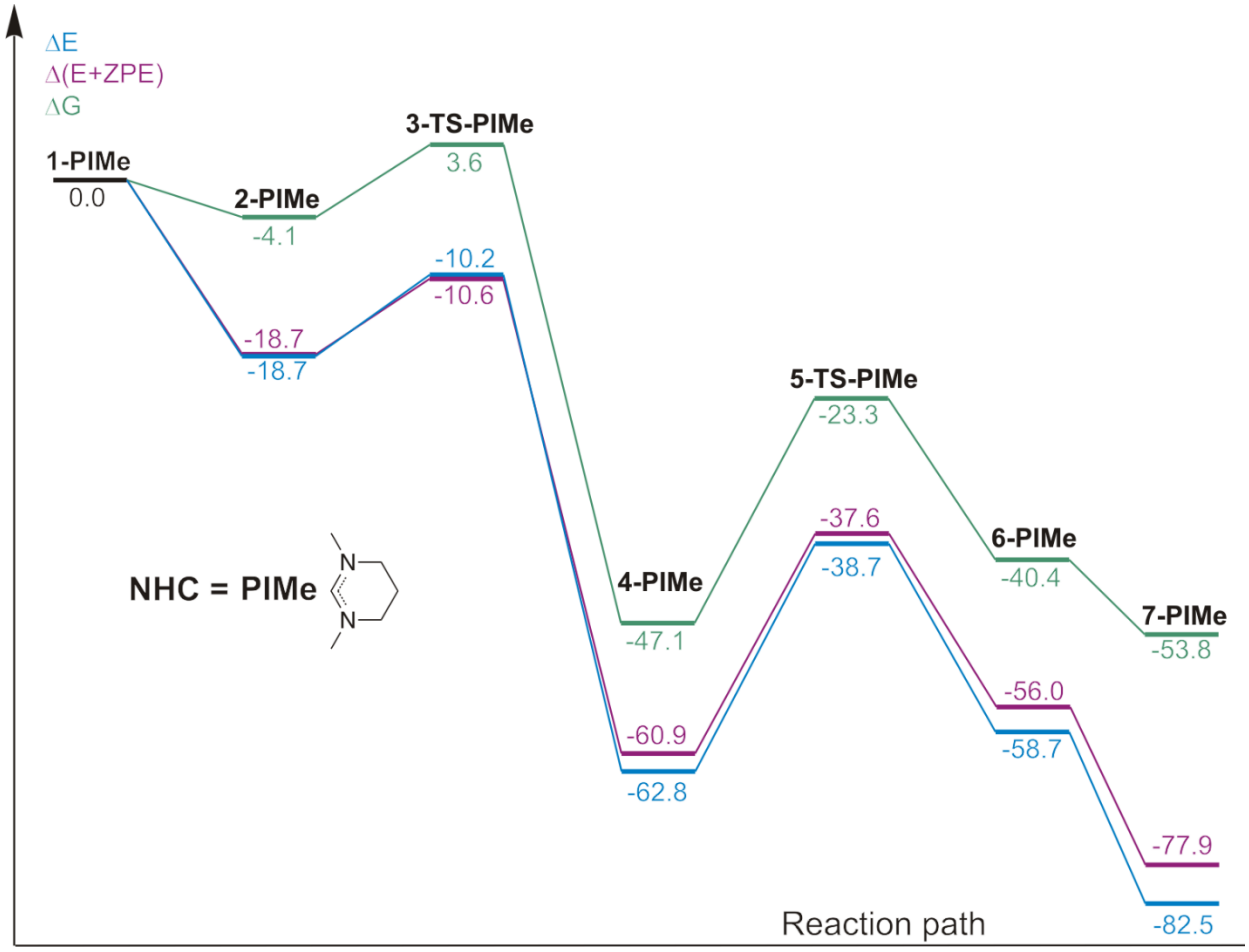

Figure S13. ΔE, Δ(E+ZPE) and ΔG potential energy surfaces for the PhI oxidative addition and subsequent Ph-NHC coupling for the **PIMe** complexes. PBE1PBE/6-311+G(d)&SDD level of theory.

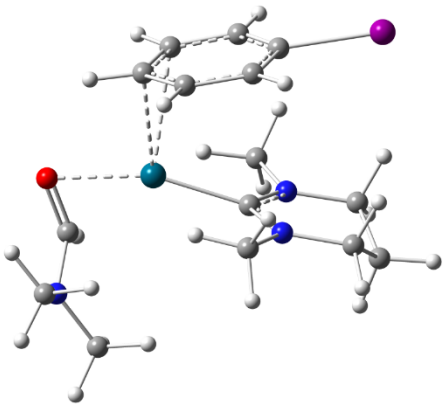

2a-PIMe

ΔE = 0; Δ(E+ZPE) = 0; ΔG = 0 kcal/mol

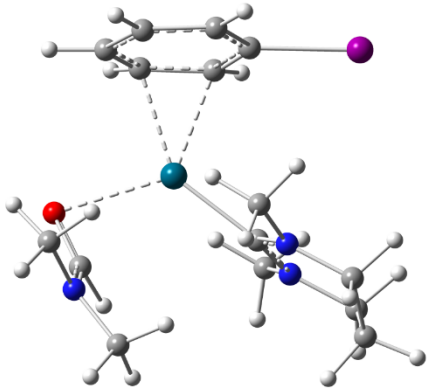

2b-PIMe

ΔE = -1.2; Δ(E+ZPE) = -1.5; ΔG = -1.3 kcal/mol

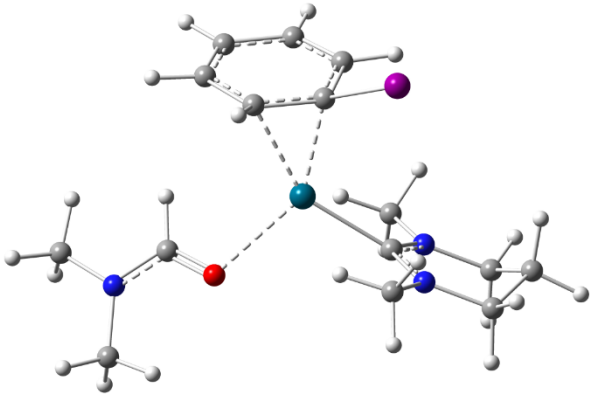

2c-PIMe

ΔE = 0.8; Δ(E+ZPE) = 0.5; ΔG = -0.9 kcal/mol

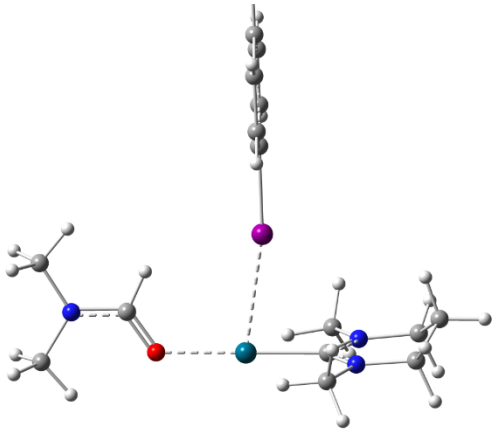

2d-PIMe

ΔE = 2.5; Δ(E+ZPE) = 2.7; ΔG = -0.3 kcal/mol

Figure S14. Energies and optimized structures of **2-PIMe** isomers.

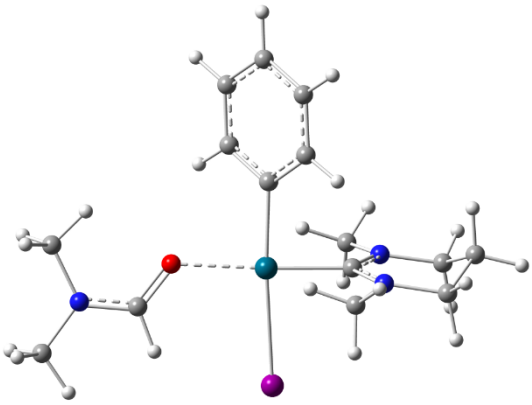

4a-PIMe

ΔE = 0; Δ(E+ZPE) = 0; ΔG = 0 kcal/mol

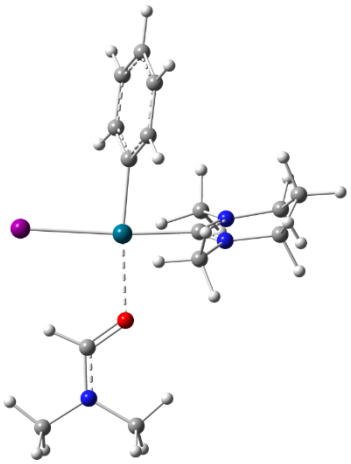

4b-PIMe

ΔE = 4.9; Δ(E+ZPE) = 4.7; ΔG = 4.9 kcal/mol

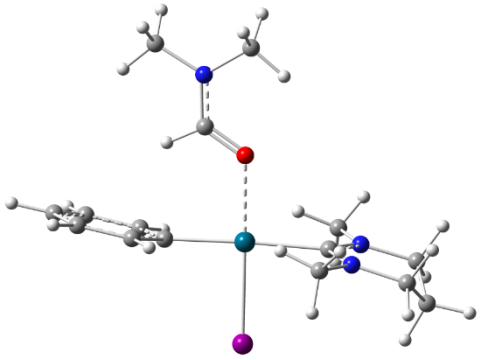

4c-PIMe

ΔE = 15.0; Δ(E+ZPE) = 14.4; ΔG = 13.4 kcal/mol

Figure S15. Energies and optimized structures of **4-PIMe** isomers.

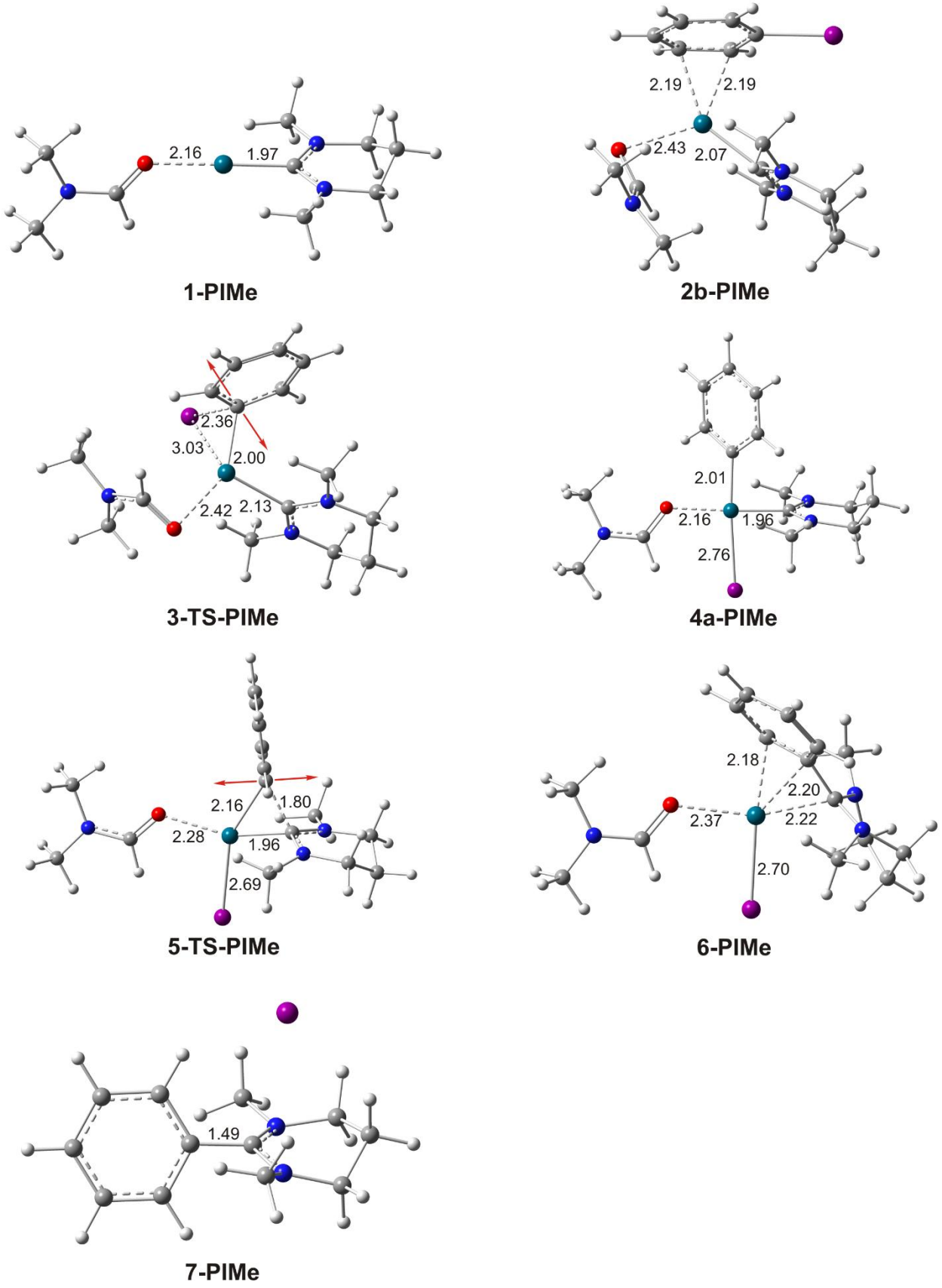

Figure S16. Optimized structures and selected bond distances (in angstroms) for **1-PIMe** – **7-PIMe** complexes. The atomic movements corresponding to the imaginary frequencies are depicted by red arrows.

***DIMe** complexes*

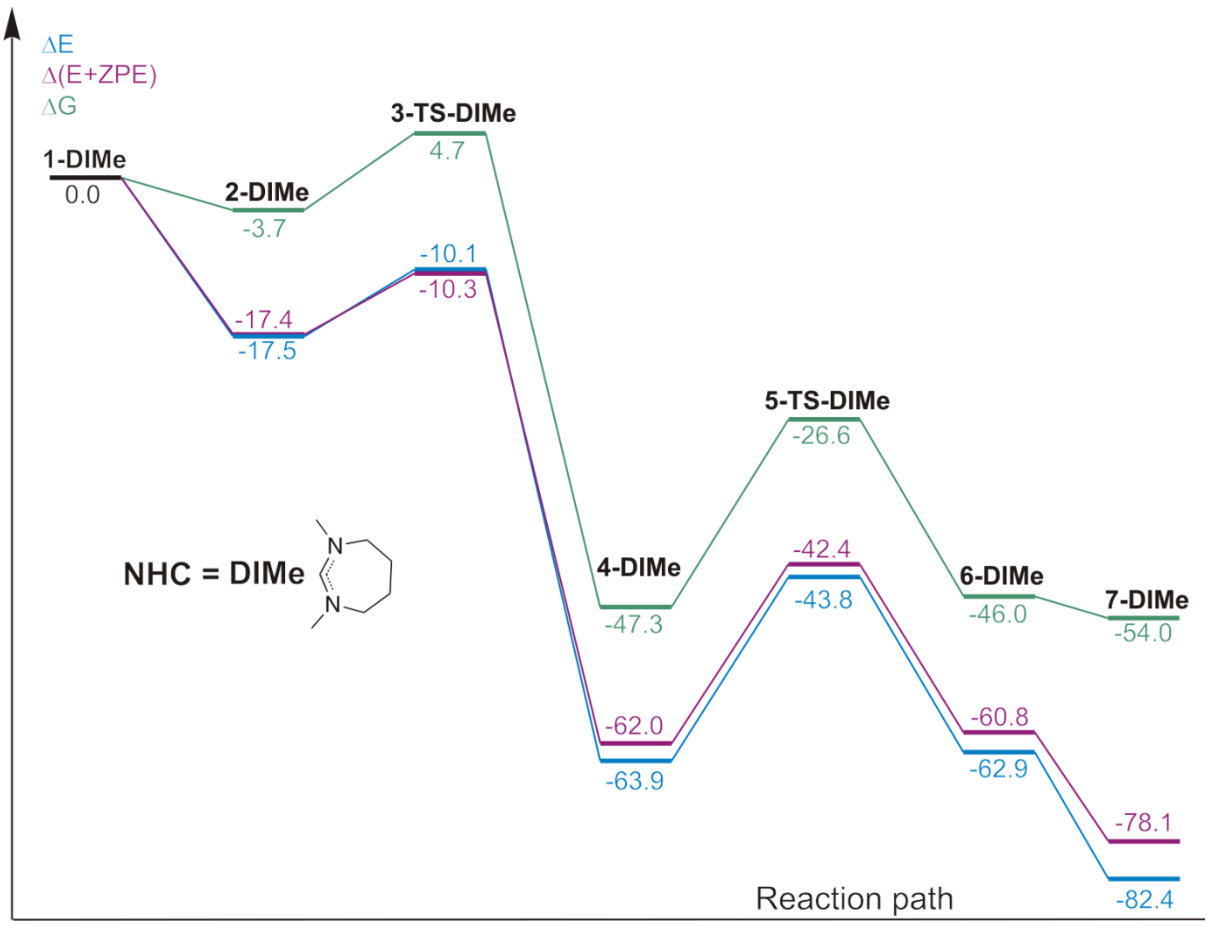

Figure S17. ΔE, Δ(E+ZPE) and ΔG potential energy surfaces for the PhI oxidative addition and subsequent Ph-NHC coupling for the **DIMe** complexes. PBE1PBE/6-311+G(d)&SDD level of theory.

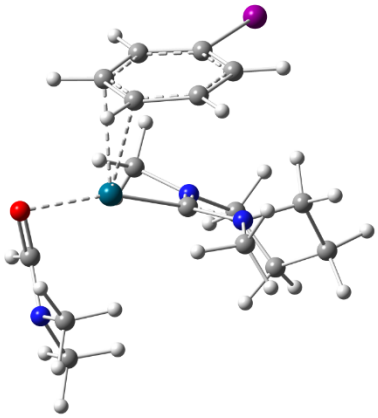

2a-DIMe

ΔE = 0; Δ(E+ZPE) = 0; ΔG = 0 kcal/mol

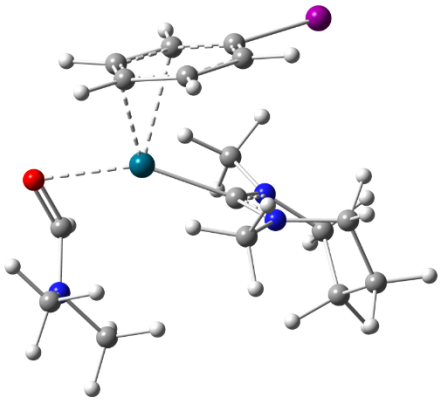

2b-DIMe

ΔE = 0; Δ(E+ZPE) = 0; ΔG = -0.5 kcal/mol

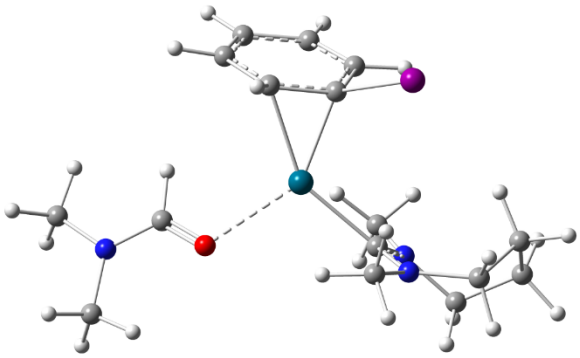

2c-DIMe

ΔE = -0.3; Δ(E+ZPE) = -0.5; ΔG = -2.0 kcal/mol

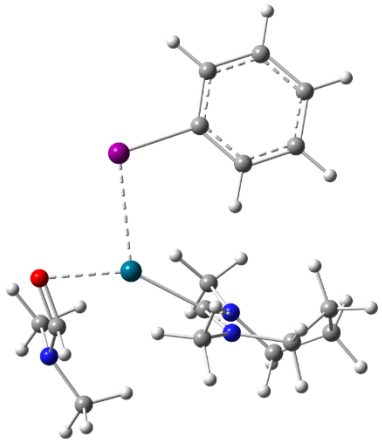

2d-DIMe

ΔE = 4.2; Δ(E+ZPE) = 4.0; ΔG = 2.4 kcal/mol

Figure S18. Energies and optimized structures of **2-DIMe** isomers.

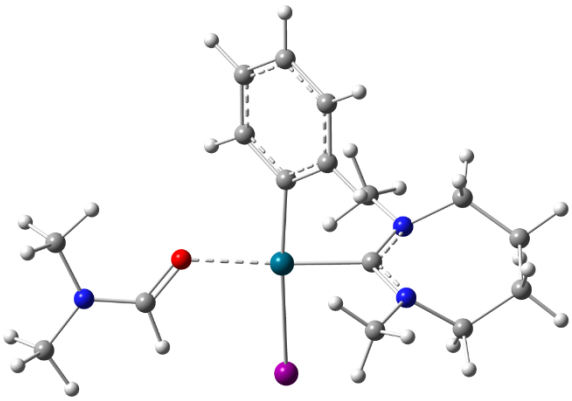

4a-DIMe

ΔE = 0; Δ(E+ZPE) = 0; ΔG = 0 kcal/mol

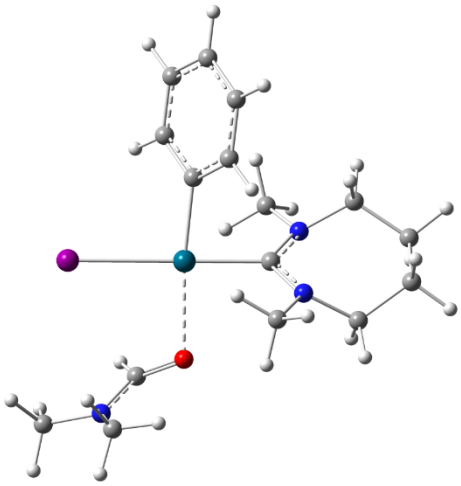

4b-DIMe

ΔE = 6.1; Δ(E+ZPE) = 6.0; ΔG = 6.4 kcal/mol

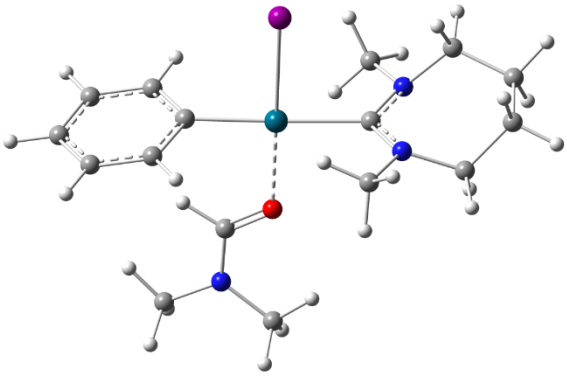

4c-DIMe

ΔE = 16.6; Δ(E+ZPE) = 16.0; ΔG = 14.8 kcal/mol

Figure S19. Energies and optimized structures of **4-DIMe** isomers.

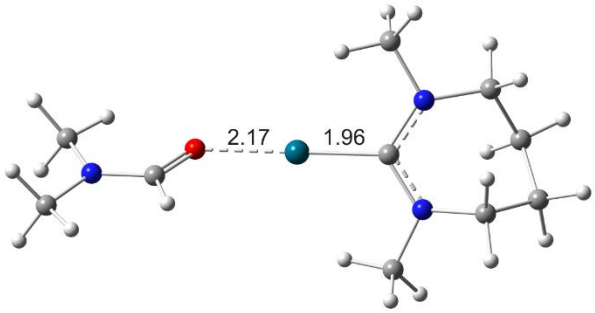

1-DIMe

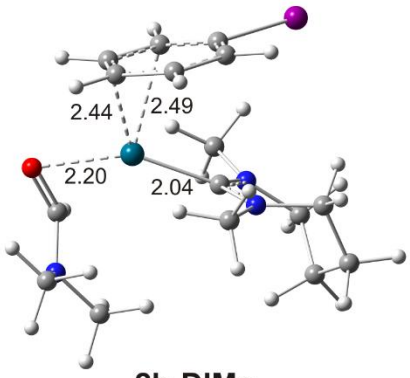

2b-DIMe

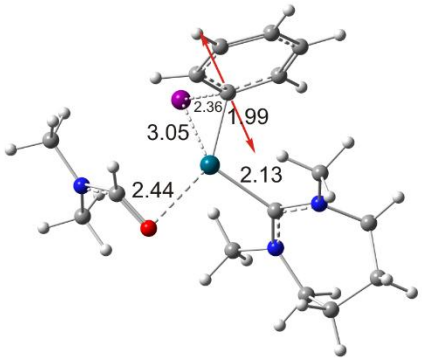

3-TS-DIMe

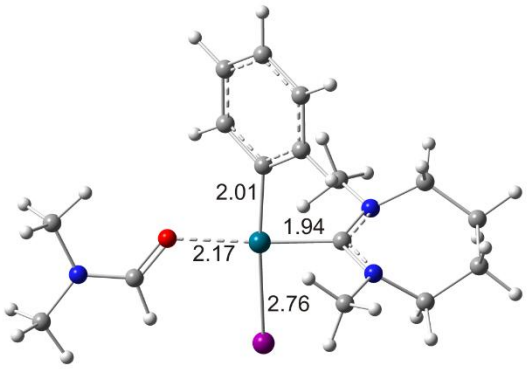

4a-DIMe

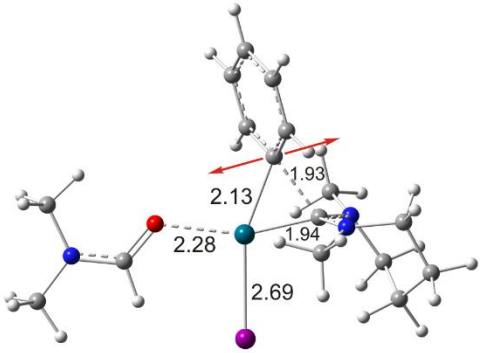

5-TS-DIMe

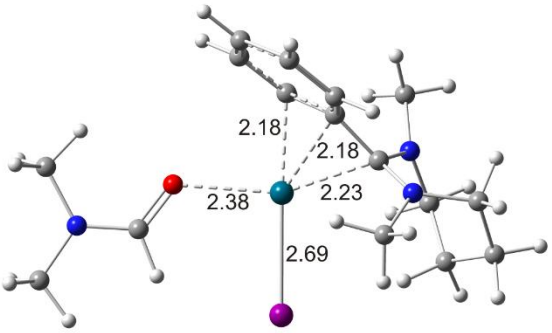

6-DIMe

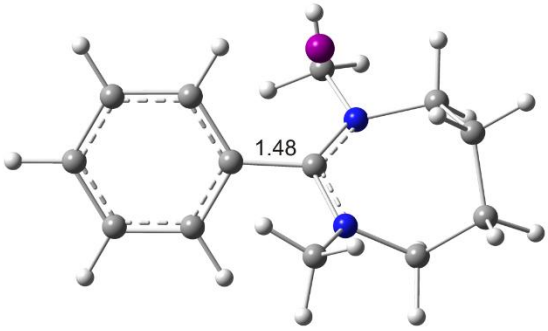

7-DIMe

Figure S20. Optimized structures and selected bond distances (in angstroms) for **1-DIMe** – **7-DIMe** complexes. The atomic movements corresponding to the imaginary frequencies are depicted by red arrows.

***IMes** complexes*

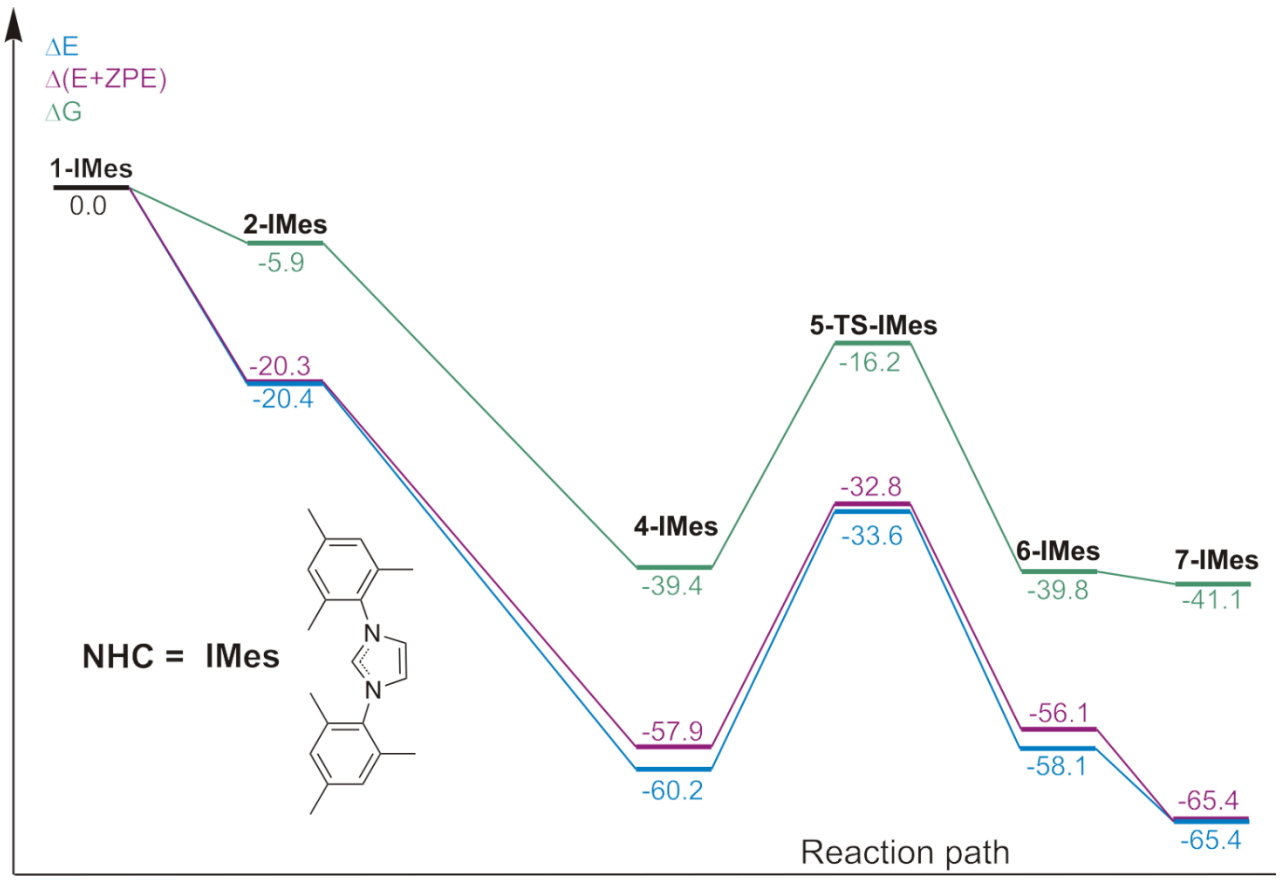

Figure S21. ΔE, Δ(E+ZPE) and ΔG potential energy surfaces for the PhI oxidative addition and subsequent Ph-NHC coupling for the **IMes** complexes (transition state **3-TS** not found). PBE1PBE/6-311+G(d)&SDD level of theory.

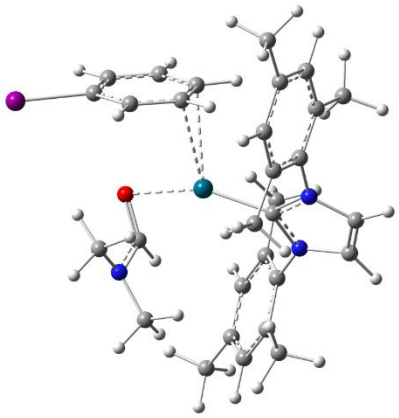

2a-IMes

ΔE = 0; Δ(E+ZPE) = 0; ΔG = 0 kcal/mol

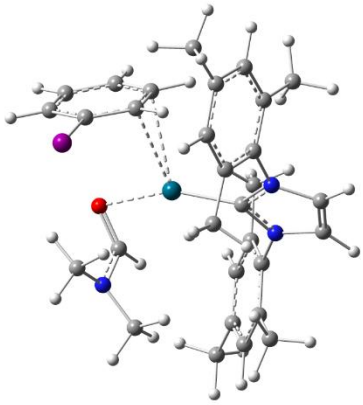

2b-IMes

ΔE = -2.2; Δ(E+ZPE) = -2.0; ΔG = -1.2 kcal/mol

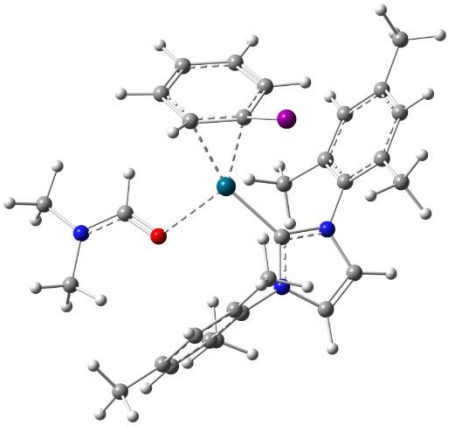

2c-IMes

ΔE = -4.3; Δ(E+ZPE) = -4.4; ΔG = -4.9 kcal/mol

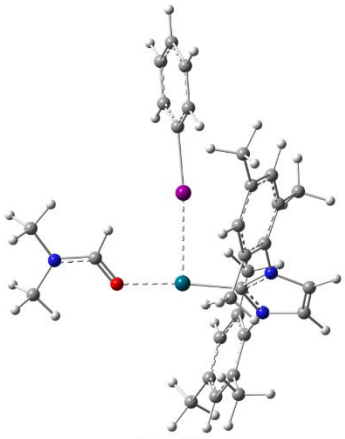

2d-IMes

ΔE = 1.0; Δ(E+ZPE) = 1.3; ΔG = -1.5 kcal/mol

Figure S22. Energies and optimized structures of **2-IMes** isomers.

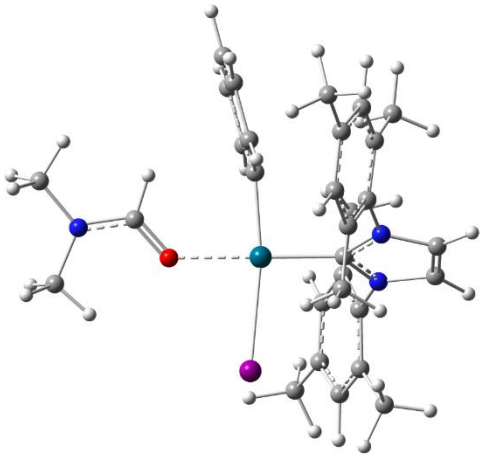

4a-IMes

ΔE = 0; Δ(E+ZPE) = 0; ΔG = 0 kcal/mol

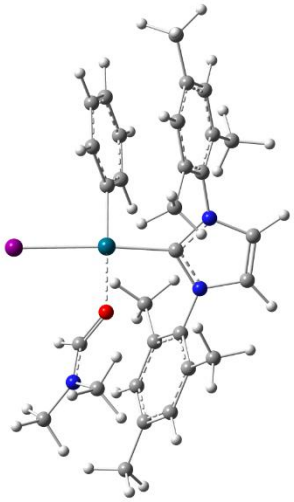

4b-IMes

ΔE = -4.1; Δ(E+ZPE) = -3.8; ΔG = -0.8 kcal/mol

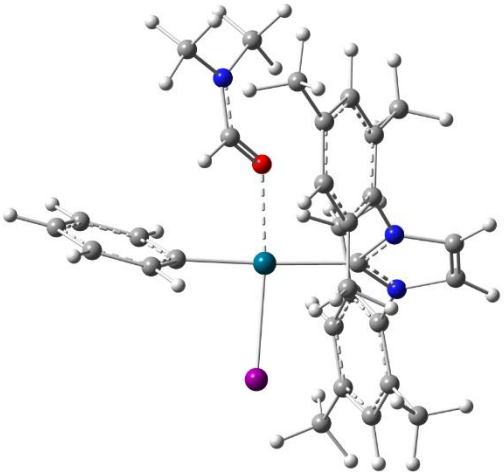

4c-IMes

ΔE = 7.0; Δ(E+ZPE) = 6.6; ΔG = 7.2 kcal/mol

Figure S23. Energies and optimized structures of **4-IMes** isomers.

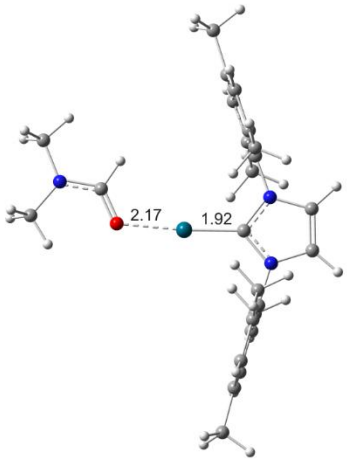

1-IMes

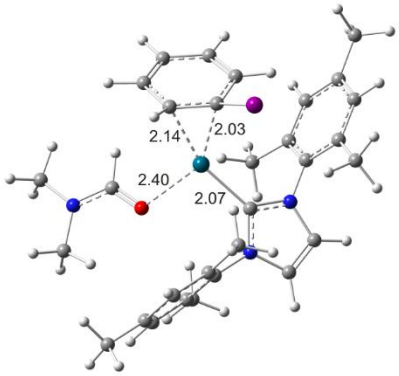

2c-IMes

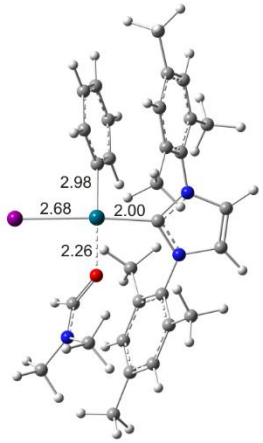

4b-IMes

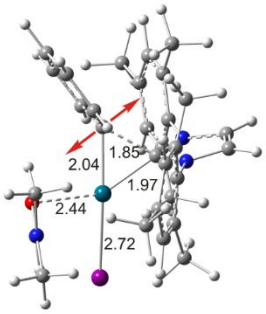

5-TS-IMes

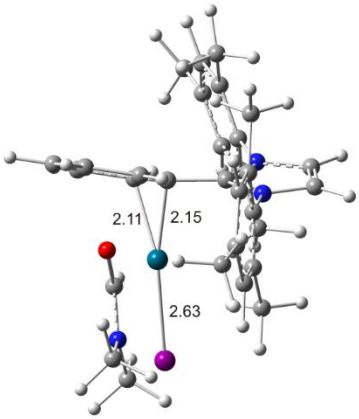

6-IMes

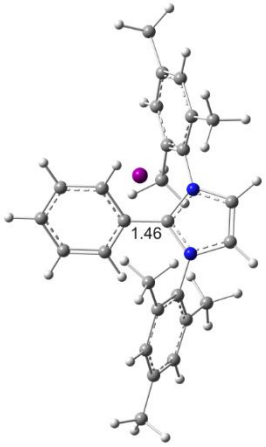

7-IMes

Figure S24. Optimized structures and selected bond distances (in angstroms) for **1-IMes** – **7-IMes** complexes (**3-TS** structure not found). The atomic movements corresponding to the imaginary frequencies are depicted by red arrows.

***IPr** complexes*

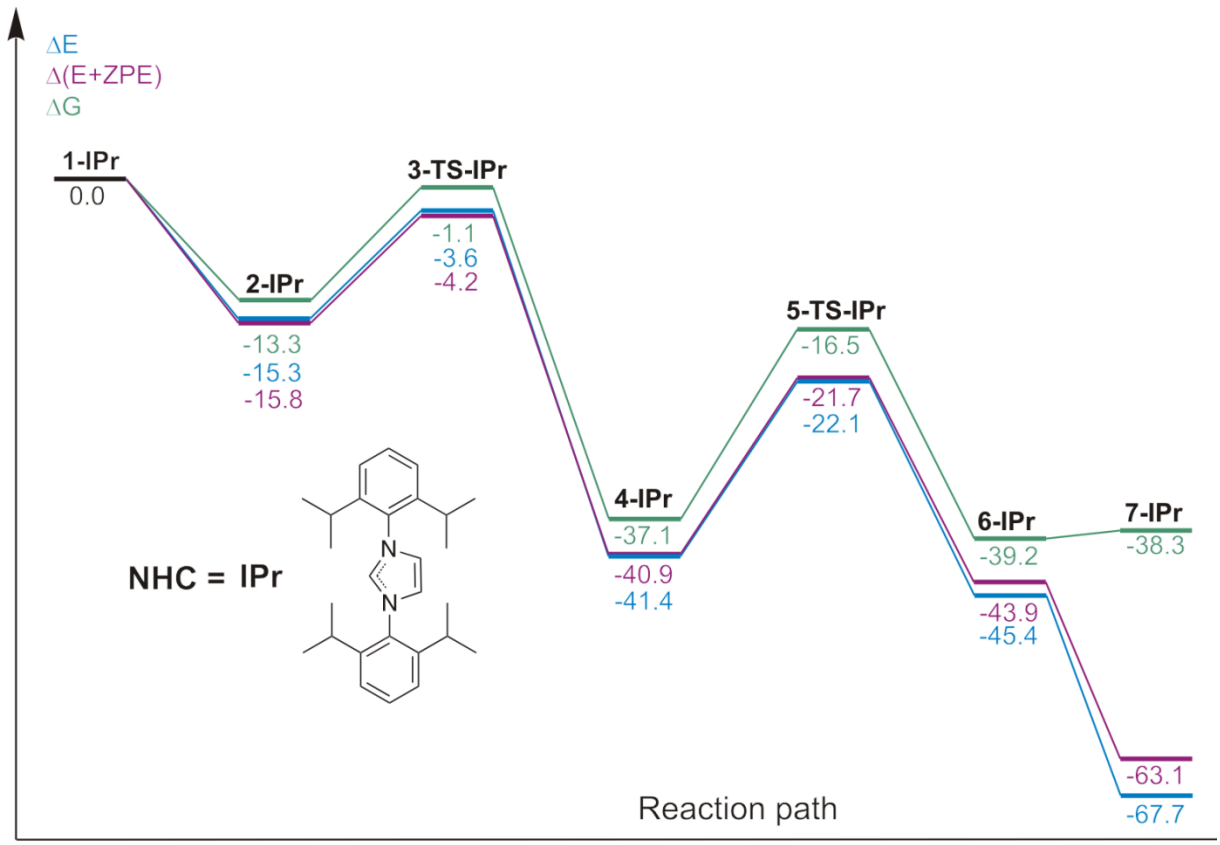

Figure S25. ΔE, Δ(E+ZPE) and ΔG potential energy surfaces for the PhI oxidative addition and subsequent Ph-NHC coupling for the **IPr** complexes. PBE1PBE/6-311+G(d)&SDD level of theory.

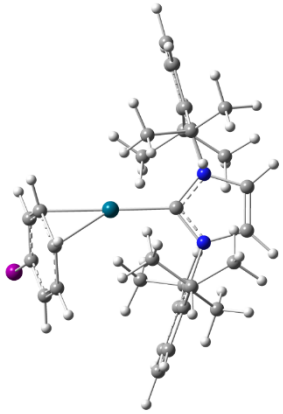

2a-IPr

ΔE = 0; Δ(E+ZPE) = 0; ΔG = 0 kcal/mol

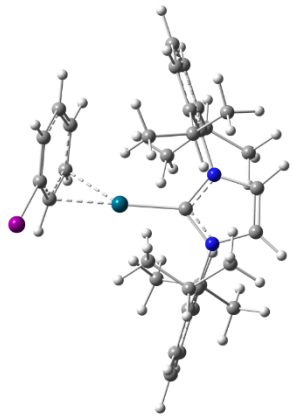

2b-IPr

ΔE = 0.1; Δ(E+ZPE) = 0; ΔG = -0.1 kcal/mol

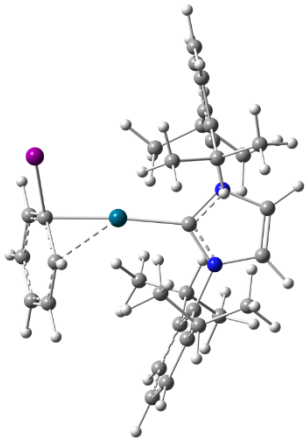

2c-IPr

ΔE = -1.8; Δ(E+ZPE) = -2.0; ΔG = -2.5 kcal/mol

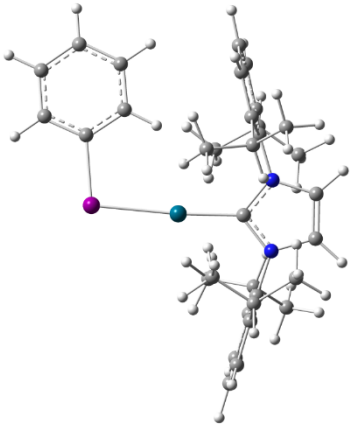

2d-IPr

ΔE = 6.2; Δ(E+ZPE) = 6.3; ΔG = 5.3 kcal/mol

Figure S26. Energies and optimized of **2-IPr** isomers.

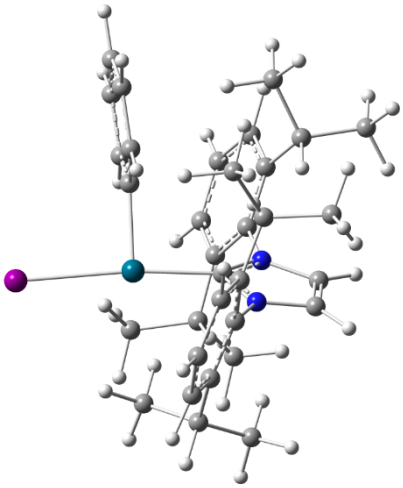

4b-IPr

ΔE = 0; Δ(E+ZPE) = 0; ΔG = 0 kcal/mol

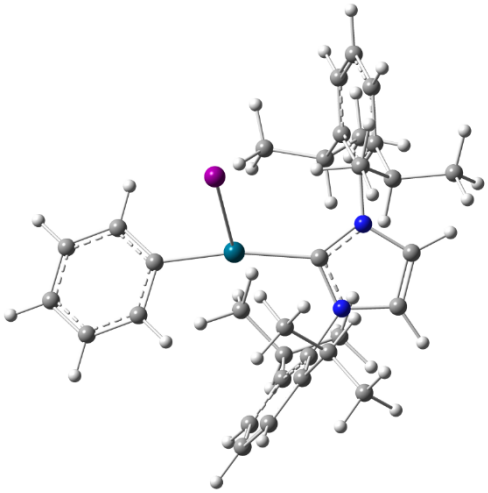

4c-IPr

ΔE = 11.8; Δ(E+ZPE) = 11.0; ΔG = 8.8 kcal/mol

Figure S27. Energies and optimized structures of **4-IPr** isomers.

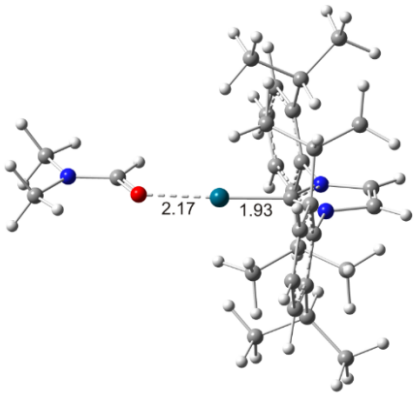

1-IPr

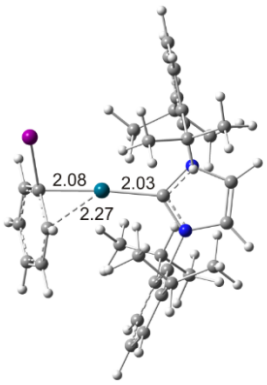

2c-IPr

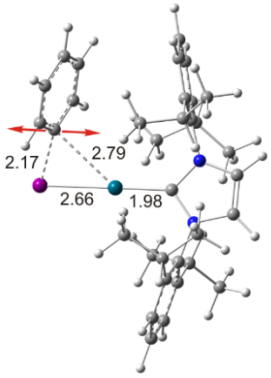

3-TS-IPr

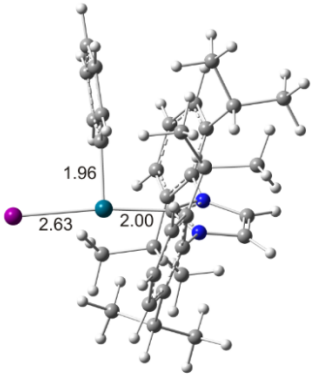

4b-IPr

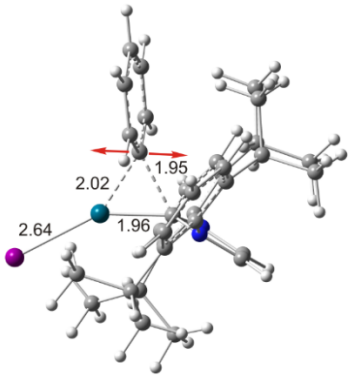

5-TS-IPr

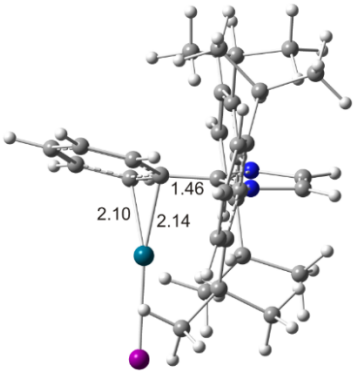

6-IPr

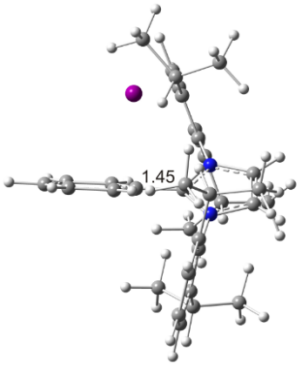

7-IPr

Figure S28. Optimized structures and selected bond distances (in angstroms) for **1-IPr** – **7-IPr** complexes. The atomic movements corresponding to the imaginary frequencies are depicted by red arrows.

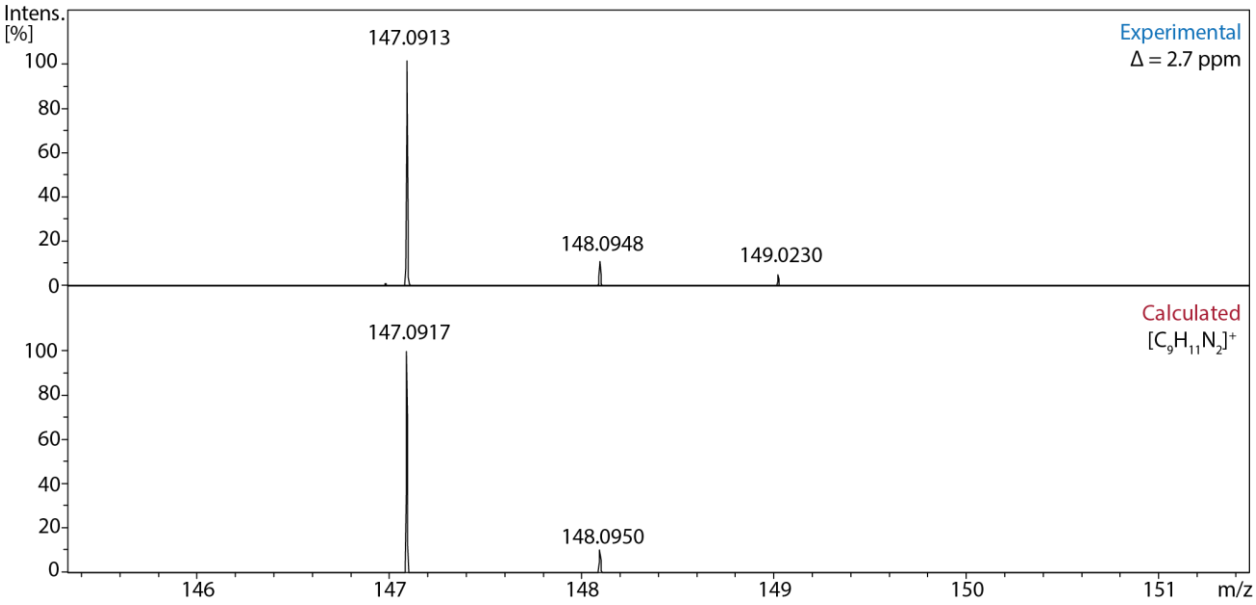

Figure S29. ESI-(+)MS spectrum of DMF solution of **8** with PhI diluted in CH_3CN, expanded to the $[C_9H_{11}N_2]^+$ region at zero point of the reaction.

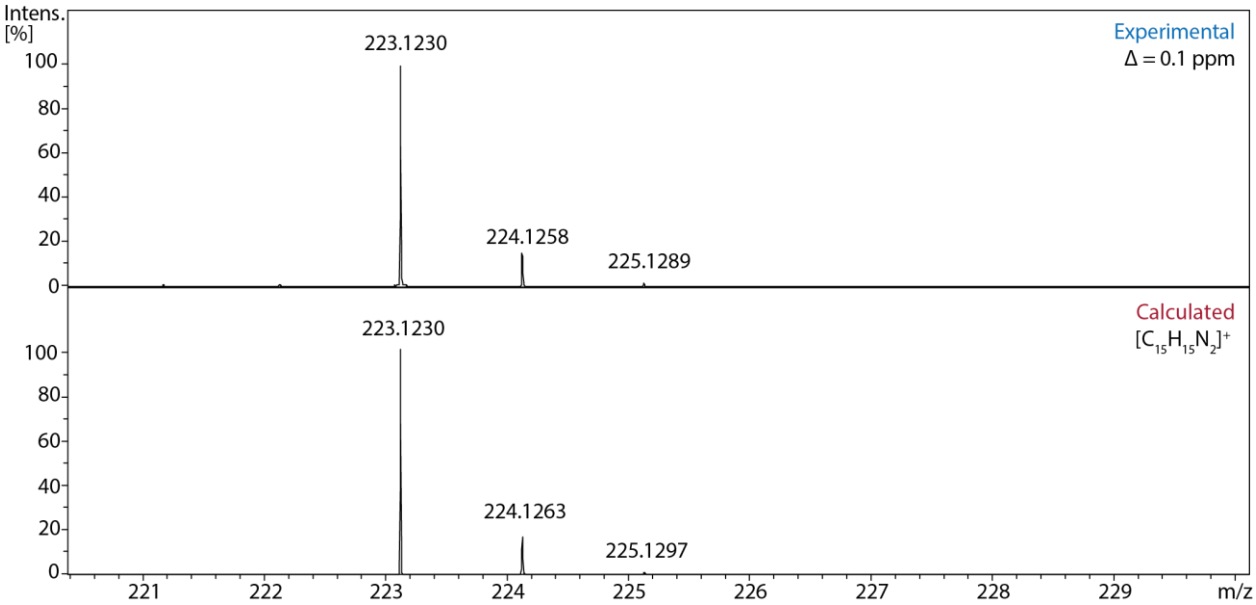

Figure S30. ESI-(+)MS spectrum of DMF solution of **8** with PhI diluted in CH_3CN, expanded to the $[C_{15}H_{15}N_2]^+$ region after reaction time of 2 h.

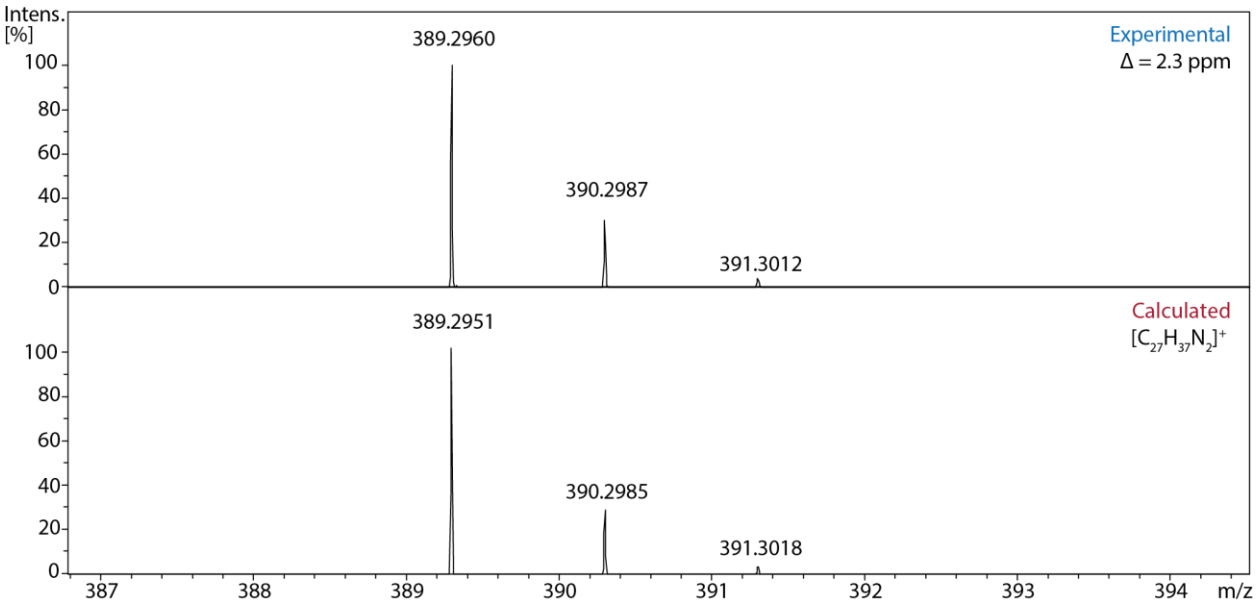

Figure S31. ESI-(+)MS spectrum of DMF solution of **9-IPr** with PhI diluted in CH_3CN, expanded to the $[C_{27}H_{37}N_2]^+$ region at zero point of the reaction.

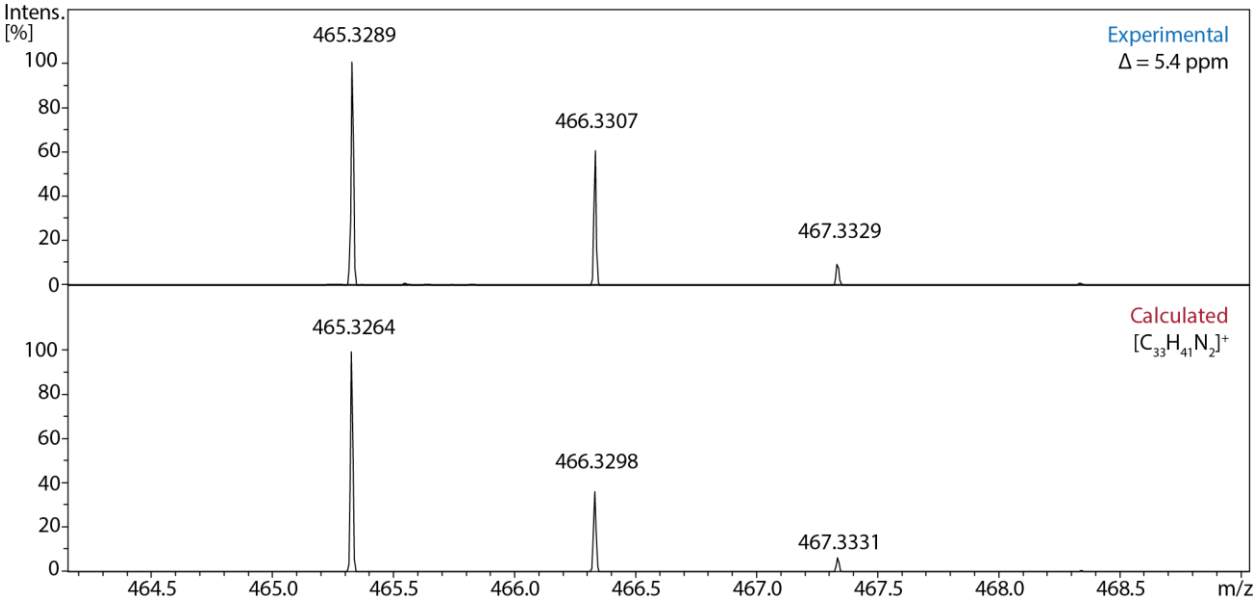

Figure S32. ESI-(+)MS spectrum of DMF solution of **9-IPr** with PhI diluted in CH_3CN, expanded to the $[C_{33}H_{41}N_2]^+$ region after reaction time of 2 h.

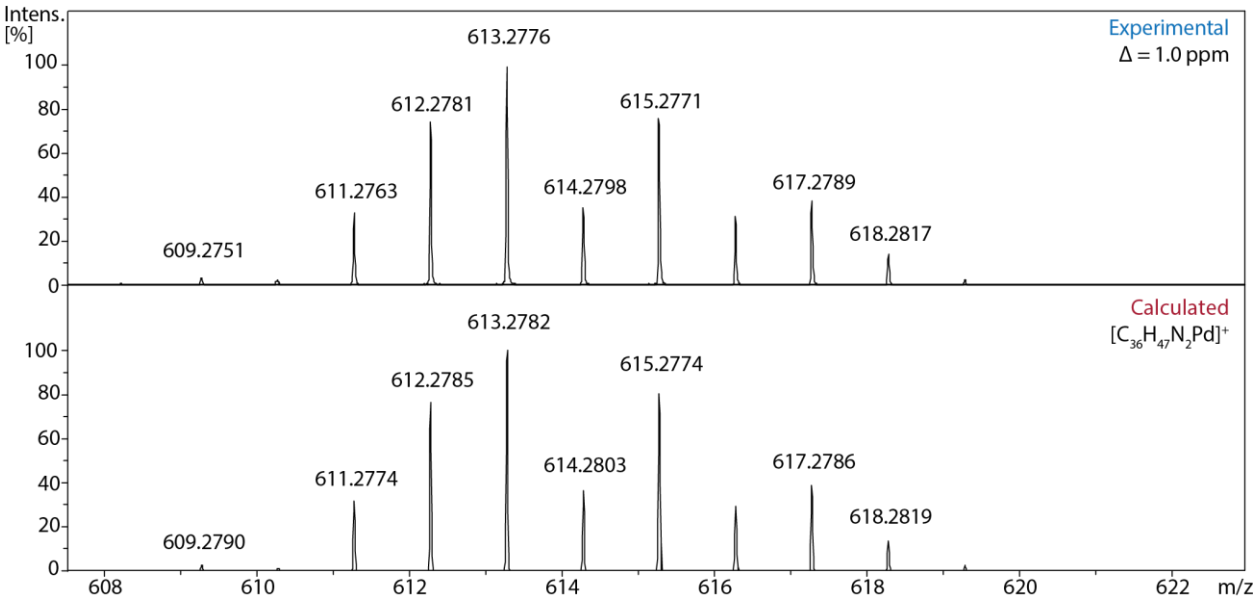

Figure S33. ESI-(+)MS spectrum of DMF solution of **9-SIPr** with PhI diluted in CH_3CN, expanded to the $[C_{36}H_{47}N_2Pd]^+$ region at zero point of the reaction.

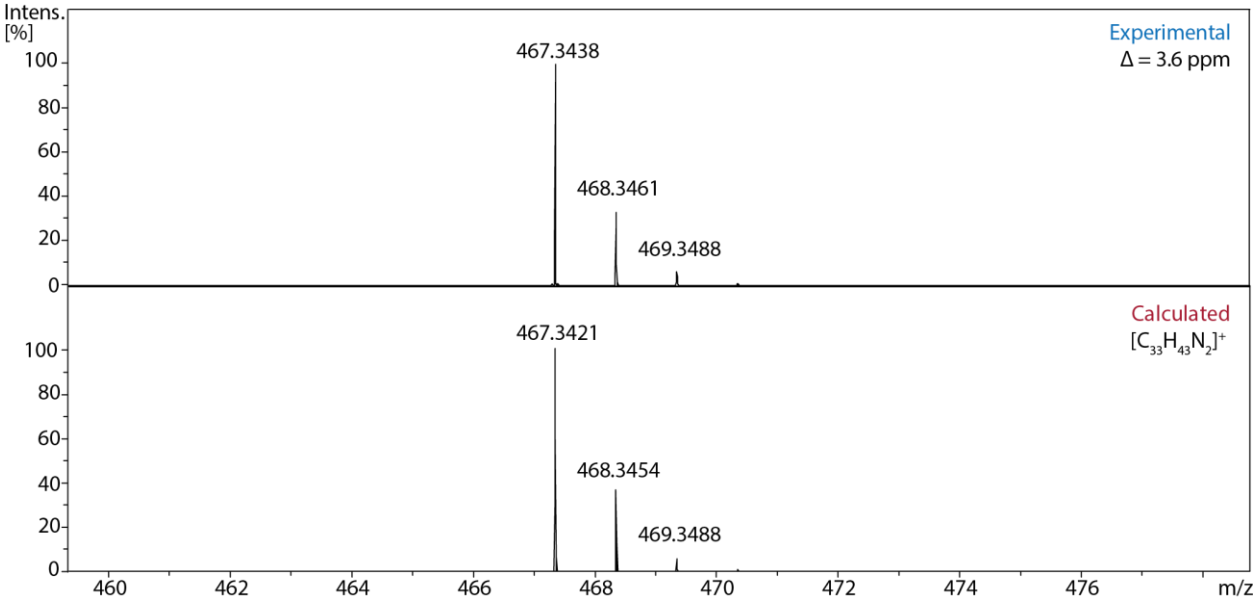

Figure S34. ESI-(+)MS spectrum of DMF solution of **9-SIPr** with PhI diluted in CH_3CN, expanded to the $[C_{33}H_{43}N_2]^+$ region after reaction time of 2 h.

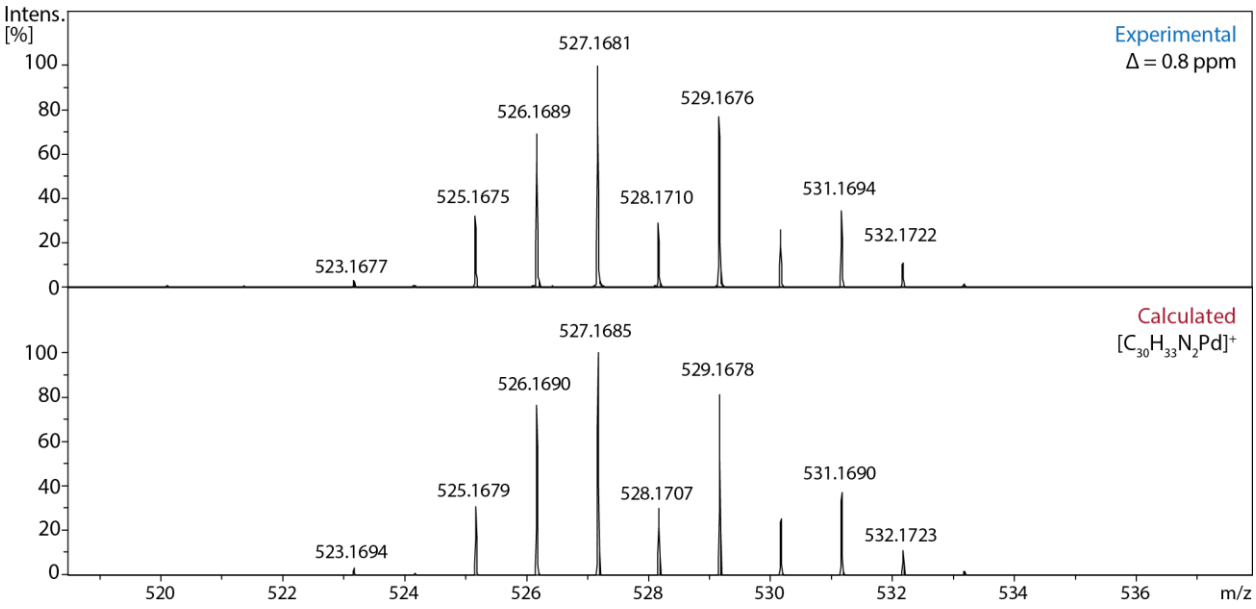

Figure S35. ESI-(+)MS spectrum of DMF solution of **9-IMes** with PhI diluted in CH_3CN, expanded to the $[C_{30}H_{33}N_2Pd]^+$ region at zero point of the reaction.

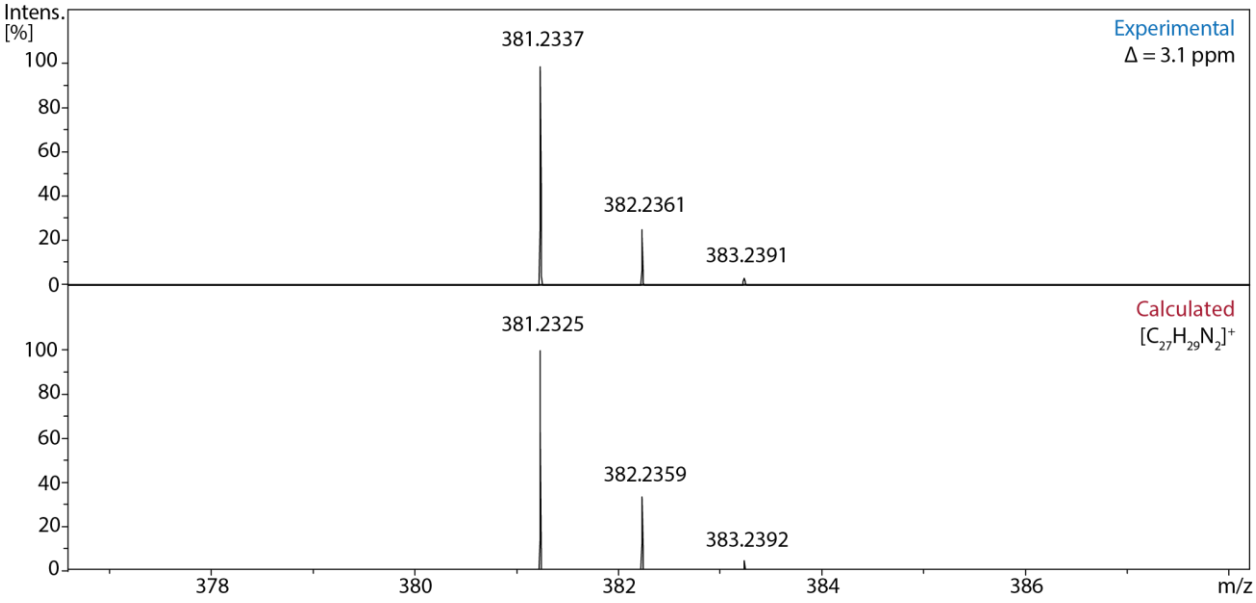

Figure S36. ESI-(+)MS spectrum of DMF solution of **9-IMes** with PhI diluted in CH_3CN, expanded to the $[C_{27}H_{29}N_2]^+$ region after reaction time of 2 h.

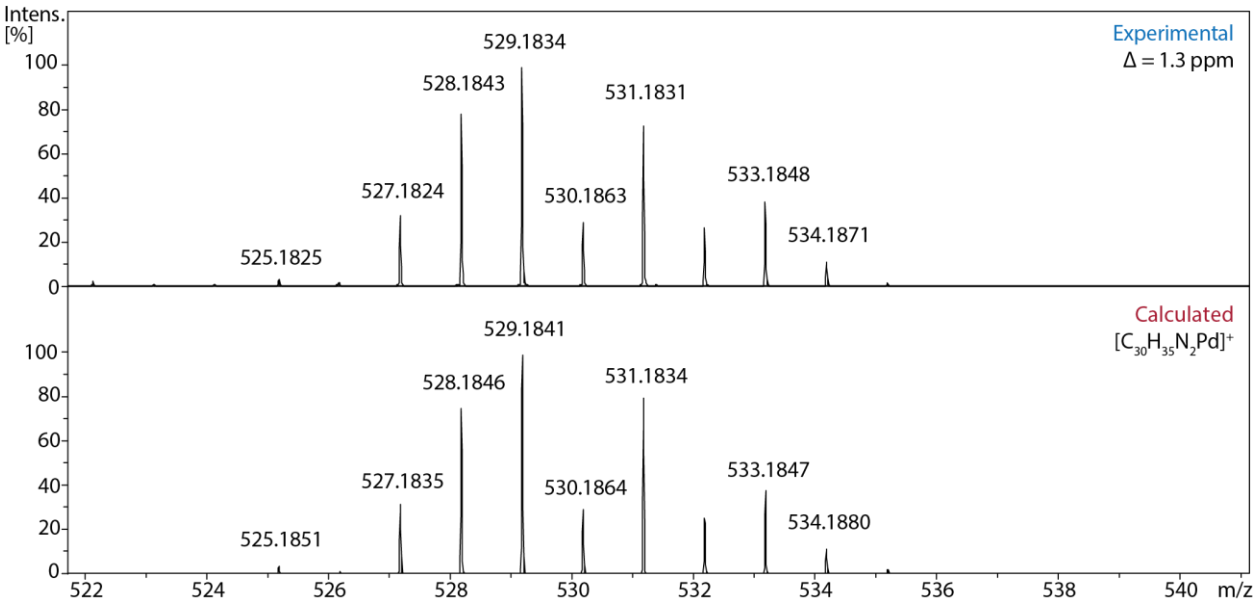

Figure S37. ESI-(+)MS spectrum of DMF solution of **9-SIMes** with PhI diluted in CH_3CN, expanded to the $[C_{30}H_{35}N_2Pd]^+$ region at zero point of the reaction.

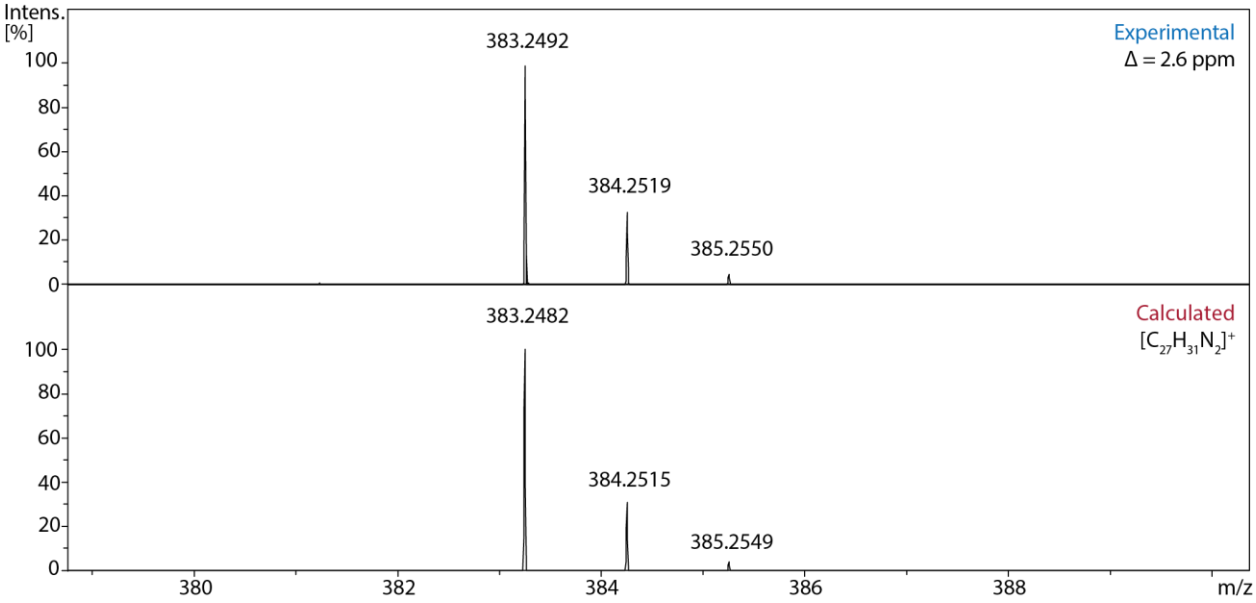

Figure S38. ESI-(+)MS spectrum of DMF solution of **9-SIMes** with PhI diluted in CH_3CN, expanded to the $[C_{27}H_{31}N_2]^+$ region after reaction time of 2 h.

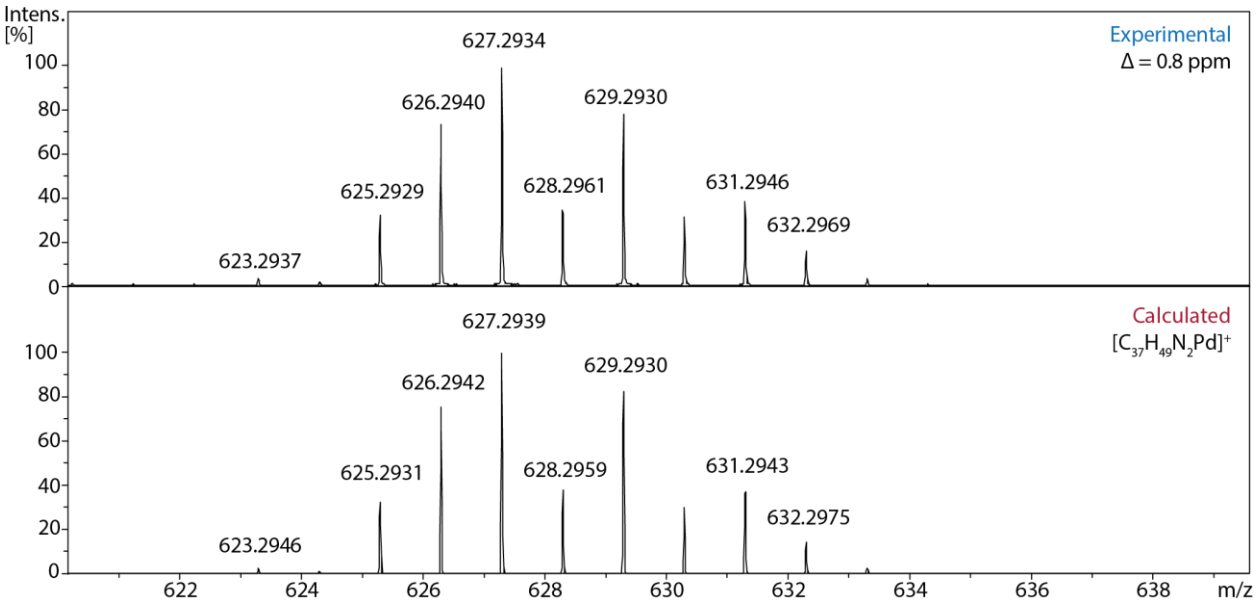

Figure S39. ESI-(+)MS spectrum of DMF solution of **9-PIPr** with PhI diluted in CH_3CN, expanded to the $[C_{37}H_{49}N_2Pd]^+$ region at zero point of the reaction.

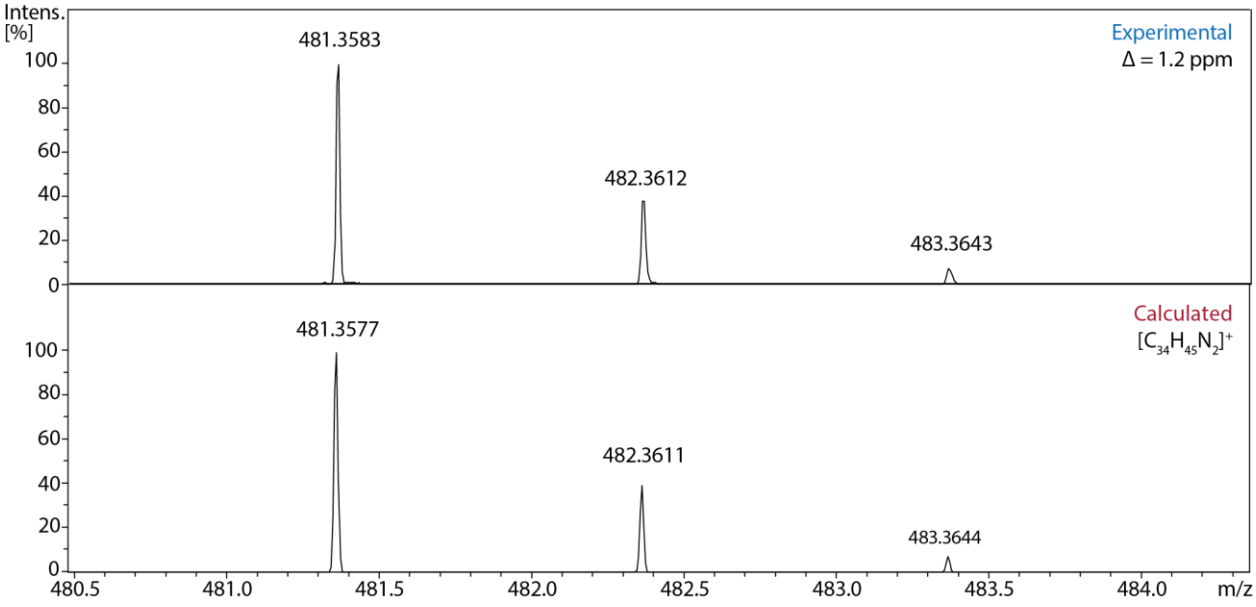

Figure S40. ESI-(+)MS spectrum of DMF solution of **9- PIPr** with PhI diluted in CH_3CN, expanded to the $[C_{34}H_{45}N_2]^+$ region after reaction time of 2 h.

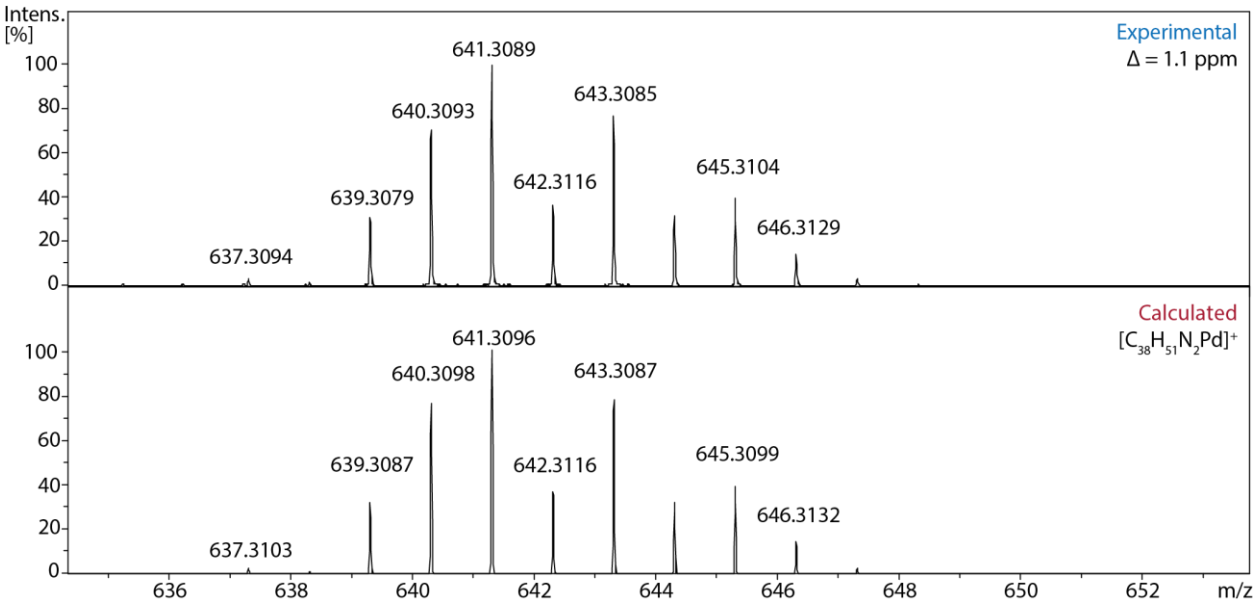

Figure S41. ESI-(+)MS spectrum of DMF solution of **9-DIPr** with PhI diluted in CH_3CN, expanded to the $[C_{38}H_{51}N_2Pd]^+$ region at zero point of the reaction.

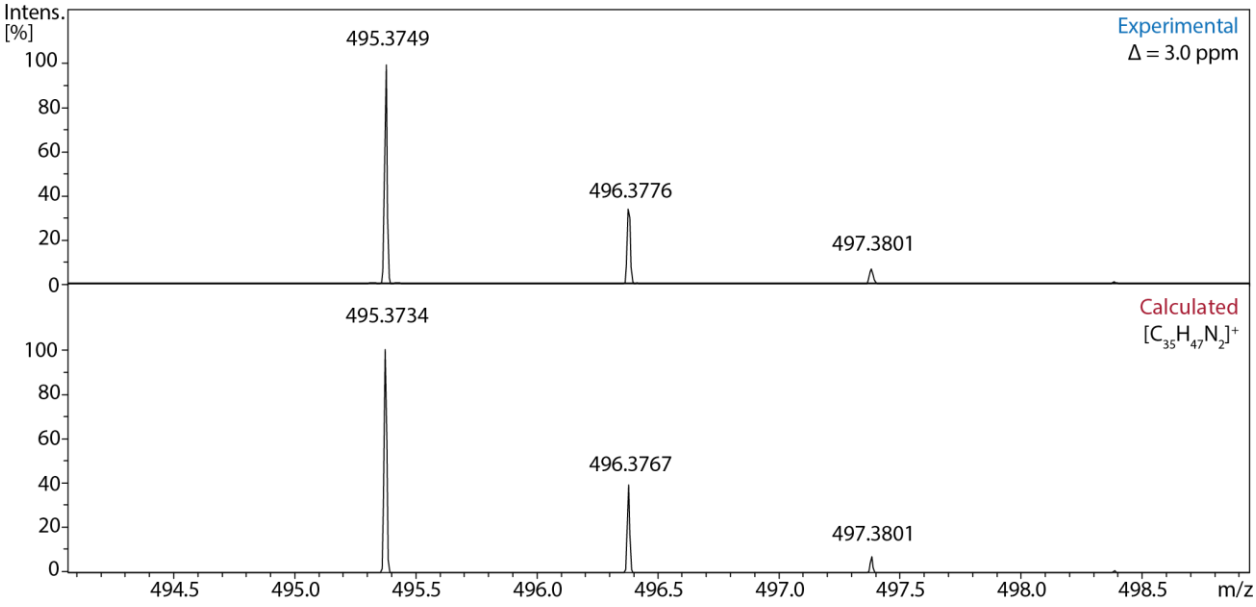

Figure S42. ESI-(+)MS spectrum of DMF solution of **9-DIPr** with PhI diluted in CH_3CN, expanded to the $[C_{35}H_{47}N_2]^+$ region after reaction time of 2 h.

Table S1. Experimental and calculated *m/z* values for cationic fragments of **7**, **8**, and **9**.

Entry	Compound	Detected form	Formula	Calculated *m/z*	Experimental *m/z*	Δ, ppm
1	**8**	H–BIMe$^+$	$C_9H_{11}N_2$	147.0917	147.0913	2.7
2	**9-IMes**	SIMes-Pd-$(C_3H_5Ph)^+$	$C_{30}H_{33}N_2Pd$	527.1685	527.1681	0.8
3	**9-SIMes**	IMes-Pd-$(C_3H_5Ph)^+$	$C_{30}H_{35}N_2Pd$	529.1841	529.1834	1.3
4	**9-SIPr**	SIPr-Pd-$(C_3H_5Ph)^+$	$C_{36}H_{47}N_2Pd$	613.2782	613.2776	1.0
5	**9-IPr**	H–IPr$^+$	$C_{27}H_{37}N_2$	389.2951	389.2960	2.3
6	**9-PIPr**	PIPr-Pd-$(C_3H_5Ph)^+$	$C_{37}H_{49}N_2Pd$	627.2939	627.2934	0.8
7	**9-DIPr**	DIPr-Pd-$(C_3H_5Ph)^+$	$C_{38}H_{51}N_2Pd$	641.3096	641.3089	1.1
1'	**7-BIMe**	Ph–BIMe$^+$	$C_{15}H_{15}N_2$	223.1230	223.1230	0.1
2'	**7-IMes**	Ph–IMes$^+$	$C_{27}H_{31}N_2$	381.2325	381.2337	3.1
3'	**7-SIMes**	Ph–SIMes$^+$	$C_{27}H_{33}N_2$	383.2482	383.2492	2.6
4'	**7-SIPr**	Ph–SIPr$^+$	$C_{33}H_{43}N_2$	467.3421	467.3438	3.6
5'	**7-IPr**	Ph–IPr$^+$	$C_{33}H_{41}N_2$	465.3264	465.3289	5.4
6'	**7-PIPr**	Ph–PIPr$^+$	$C_{34}H_{45}N_2$	481.3577	481.3583	1.2
7'	**7-DIPr**	Ph–DIPr$^+$	$C_{35}H_{47}N_2$	495.3734	495.3749	3.0

Table S2. Bonding in **4**, **5-TS** and **6**. Interatomic distances (ID, in Å), Wiberg bond indexes (BI), atomic charge differences (Δq), and energies of NBOs (ENBO, eV).

Bonding parameters		**BIMe**	**IMe**	**SIMe**	**PIMe**	**DIMe**	**IMes**	**IPr**
4								
ID	Pd-C_{NHC}	1.933	1.936	1.933	1.957	1.940	1.962	2.002
	Pd-C_{Ph}	2.007	2.005	2.007	2.007	2.013	2.001	1.963
	Pd-I	2.748	2.754	2.749	2.758	2.755	2.734	2.629
BI	Pd-C_{NHC}	0.71	0.70	0.69	0.68	0.70	0.68	0.56
	Pd-C_{Ph}	0.66	0.66	0.65	0.65	0.64	0.64	0.76
	Pd-I	0.63	0.62	0.62	0.62	0.62	0.64	0.8
Δq	Pd-C_{NHC}	-0.34	-0.28	-0.37	-0.41	-0.43	-0.23	-0.29
	Pd-C_{Ph}	0.22	0.24	0.23	0.20	0.22	0.31	0.01
	Pd-I	0.55	0.58	0.56	0.52	0.54	0.61	0.34
ENBO	Pd-C_{NHC}	-0.47	-0.46	-0.46	-0.43	-0.44	-0.46	-0.45
	Pd-C_{Ph}	-0.31	-0.31	-0.30	-0.30	-0.30	-0.32	-0.37
	Pd-I	-0.34	-0.34	-0.34	-0.35	-0.35	-0.33	-0.36
5-TS								
ID	Pd-C_{NHC}	1.926	1.936	1.925	1.957	1.937	1.973	1.961
	Pd-C_{Ph}	2.113	2.114	2.124	2.155	2.130	2.038	2.016
	Pd-I	2.687	2.700	2.686	2.687	2.694	2.721	2.640
	C_{Ph}-C_{NHC}	1.842	1.815	1.860	1.797	1.934	1.850	1.945
BI	Pd-C_{NHC}	0.63	0.59	0.63	0.62	0.61	0.56	0.54
	Pd-C_{Ph}	0.37	0.37	0.36	0.32	0.35	0.40	0.45
	Pd-I	0.67	0.65	0.66	0.67	0.65	0.65	0.78
	C_{Ph}-	0.67	0.69	0.66	0.71	0.63	0.68	0.62

	C_{NHC}							
Δq	Pd-C_{NHC}	-0.39	-0.37	-0.40	-0.44	-0.46	-0.38	-0.49
	Pd-C_{Ph}	0.20	0.19	0.23	0.19	0.20	0.17	0.04
	Pd-I	0.50	0.53	0.52	0.48	0.50	0.54	0.52
	C_{Ph}-C_{NHC}	-0.60	-0.57	-0.63	-0.63	0.65	-0.55	-0.54
ENBO	Pd-C_{NHC}	-0.37	-0.04	-0.35	-0.34	-0.35	-0.37	-0.39
	C_{NHC}-Pd-C_{Ph}	-0.49	-0.30	-0.41	-0.50	-0.44	-0.59	-0.48
	Pd-I	-0.36	-0.35	-0.35	-0.35	-0.36	-0.25	-0.26
6								
ID	Pd-C_{NHC}	2.132	2.94	2.158	2.217	2.233	2.709	2.746
	Pd-C_{Ph}	2.209	2.201	2.207	2.203	2.182	2.148	2.135
	Pd-I	2.680	2.697	2.690	2.695	2.694	2.630	2.637
	C_{Ph}-C_{NHC}	1.473	1.468	1.468	1.469	1.468	1.459	1.457
BI	Pd-C_{NHC}	0.45	0.37	0.44	0.40	0.41	0.12	0.11
	Pd-C_{Ph}	0.17	0.18	0.17	0.17	0.17	0.24	0.25
	Pd-I	0.67	0.65	0.65	0.64	0.65	0.74	0.73
	C_{Ph}-C_{NHC}	1.07	1.07	1.08	1.10	1.01	1.10	1.10
Δq	Pd-C_{NHC}	-0.37	-0.40	-0.39	-0.39	-0.38	-0.67	-0.64
	Pd-C_{Ph}	0.18	0.16	0.18	0.19	0.21	0.07	0.12
	Pd-I	0.51	0.53	0.53	0.54	0.55	0.35	0.40
	C_{Ph}-C_{NHC}	0.54	0.55	0.57	0.59	0.60	0.74	0.75
ENBO	Pd-C_{NHC}	-0.29	-0.30	-0.31	-0.30	-0.30	-	-
	Pd-C_{Ph}	-0.30	-0.30	-0.30	-0.30	-0.30	-0.32	-0.32
	Pd-I	-0.36	-0.23	-0.24	-0.24	-0.24	-0.27	-0.30
	C_{Ph}-C_{NHC}	-0.70	-0.70	-0.69	0.69	-0.69	-0.73	-0.74

Characterization of Pd nanoparticles with the use of TEM and EDS

9-IMes

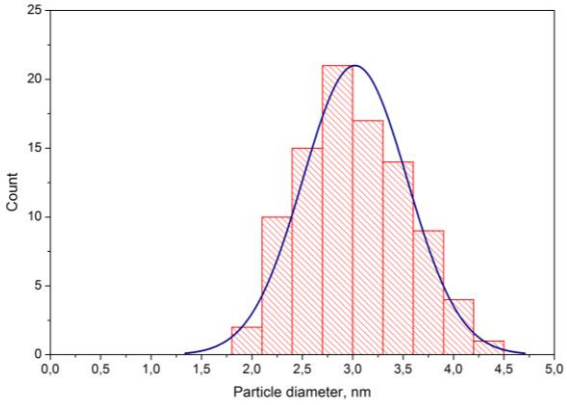

Average particles diameter: 3.02 nm
Standard deviation: 0.52 nm

9-SIPr

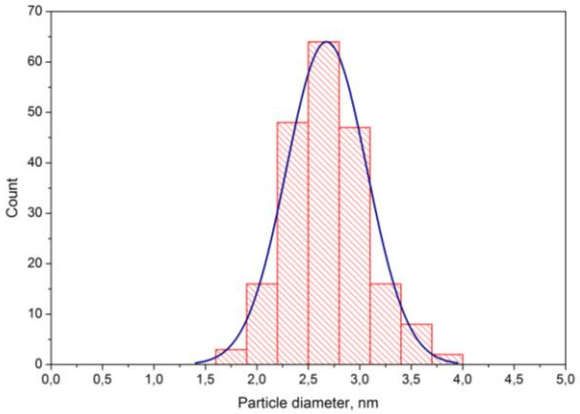

Average particles diameter: 2.68 nm
Standard deviation: 0.39 nm

9-PIPr

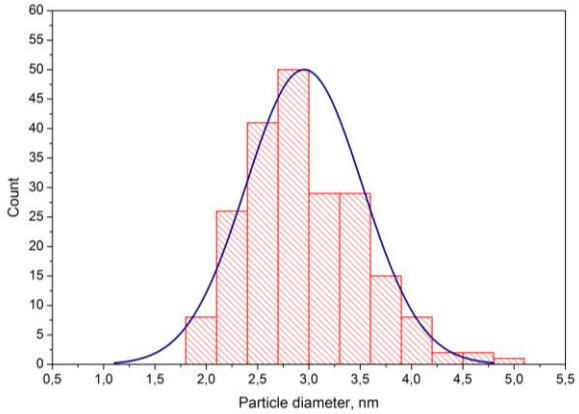

Average particles diameter: 2.95 nm
Standard deviation: 0.57 nm

9-DIPr

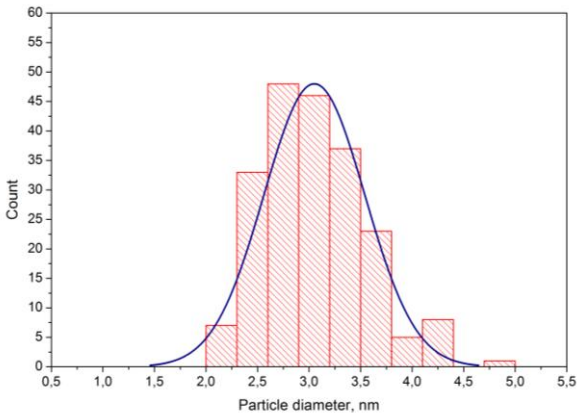

Average particles diameter: 3.05 nm
Standard deviation: 0.49 nm

Figure S43. Statistical analysis of the Pd-containing NPs formed in the reaction of **9** with iodobenzene. Histograms of particle diameter distribution (red) and corresponding normal distribution curves (blue). Average particle sizes and standard deviations are given under each graph.

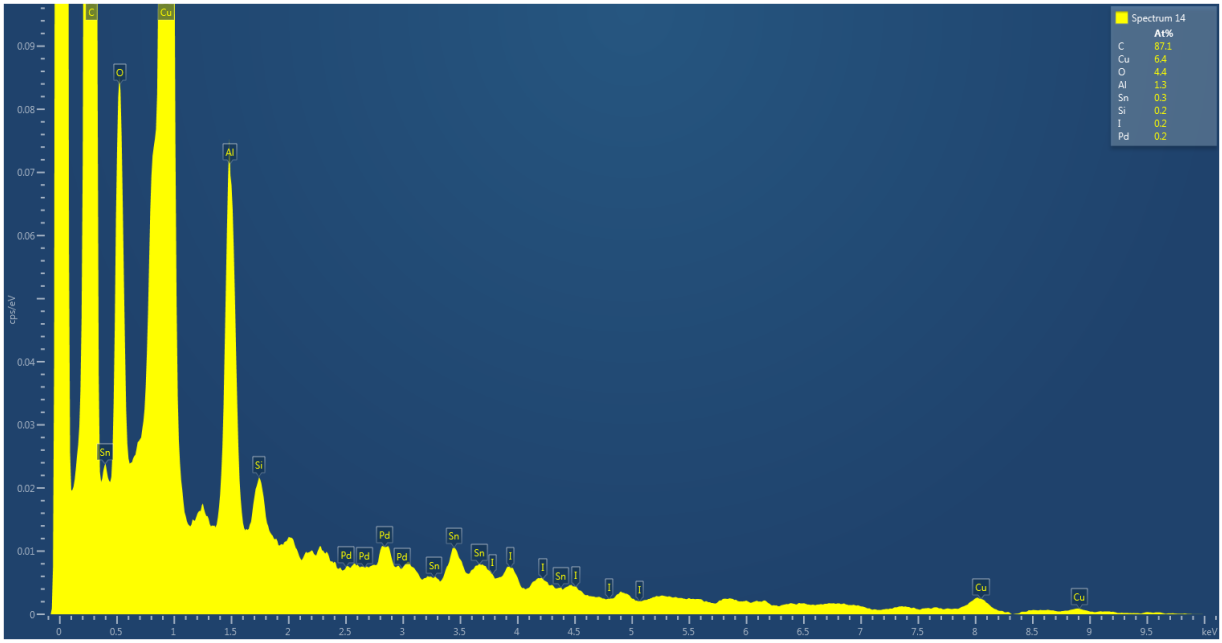

Figure S44. EDX spectrum of TEM grid containing particles obtained from **9-SIPr** complex. Spectrum was scaled and smoothed for more clear presentation of low-intensity signals.

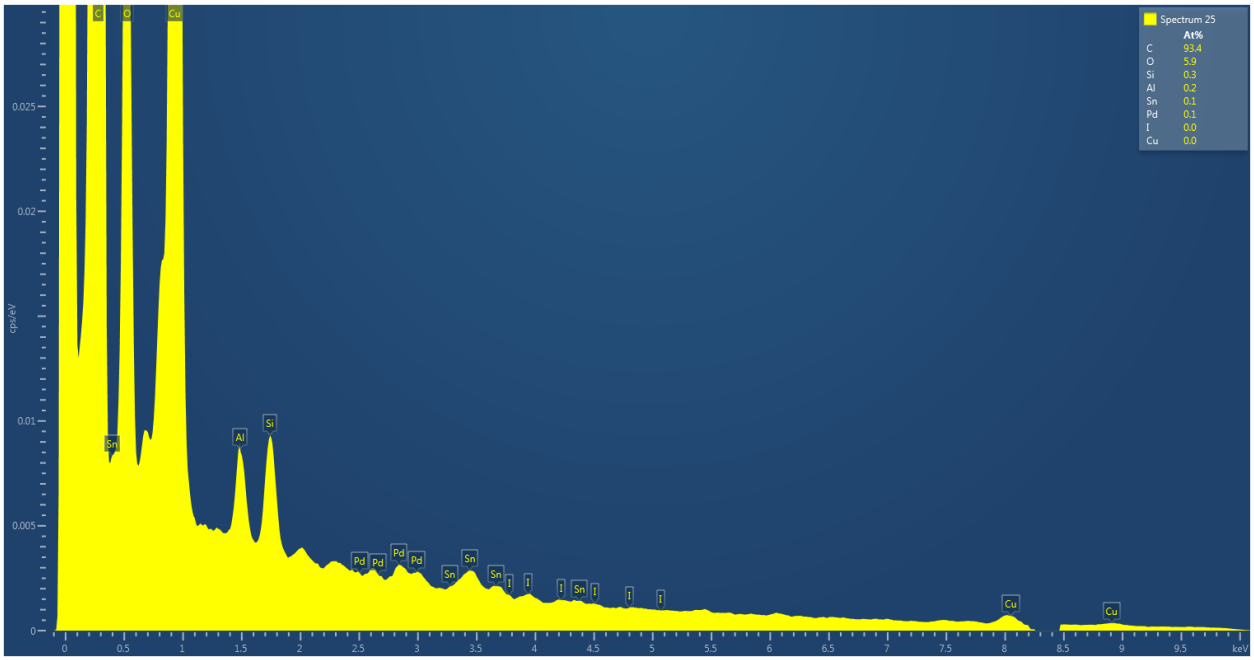

Figure S45. EDX spectrum of TEM grid containing particles obtained from **9-PIPr** complex. Spectrum was scaled and smoothed for more clear presentation of low-intensity signals.

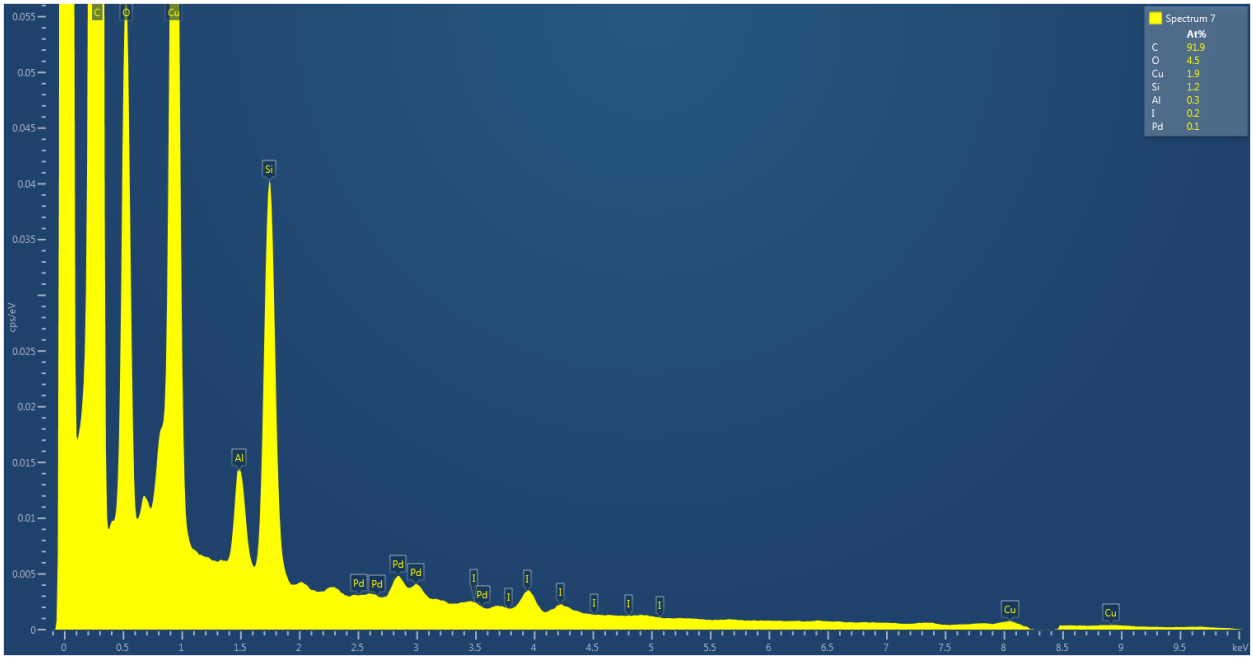

Figure S46. EDX spectrum of TEM grid containing particles obtained from **9-DIPr** complex. Spectrum was scaled and smoothed for more clear presentation of low-intensity signals.

Comment: Assignment of the signals in EDX spectra

Element(s)	Source
C, O	Carbon support on TEM grid
Cu, O, Sn	TEM grid, specimen holder
Al, O	Specimen holder
Si	Silicon drift detector (EDX spectrometer)
Pd, I	**Particles**: metallic Pd, PdI (or azolium salt for I)